

Monsoons climate change assessment

Article

Accepted Version

Wang, B., Biasutti, M., Byrne, M. P., Castro, C., Chang, C.-P., Cook, K., Fu, R., Grimm, A. M., Ha, K.-J., Hendon, H., Kitoh, A., Krishnan, R., Lee, J.-Y., Li, J., Liu, J., Moise, A., Pascale, S., Roxy, M. K., Seth, A., Sui, C.-H., Turner, A. ORCID: <https://orcid.org/0000-0002-0642-6876>, Yang, S., Yun, K.-S., Zhang, L. and Zhou, T. (2021) Monsoons climate change assessment. *Bulletin of the American Meteorological Society*, 102 (1). E1-E19. ISSN 1520-0477 doi: <https://doi.org/10.1175/BAMS-D-19-0335.1> Available at <https://centaur.reading.ac.uk/90181/>

It is advisable to refer to the publisher's version if you intend to cite from the work. See [Guidance on citing](#).

To link to this article DOI: <http://dx.doi.org/10.1175/BAMS-D-19-0335.1>

Publisher: American Meteorological Society

All outputs in CentAUR are protected by Intellectual Property Rights law, including copyright law. Copyright and IPR is retained by the creators or other copyright holders. Terms and conditions for use of this material are defined in the [End User Agreement](#).

www.reading.ac.uk/centaur

CentAUR

Central Archive at the University of Reading

Reading's research outputs online

1 Monsoons Climate Change Assessment

2

3 Bin Wang¹, Michela Biasutti², Michael P. Byrne^{3,4}, Christopher Castro⁴, Chih-Pei Chang^{5,6}, Kerry4 Cook⁷, Rong Fu⁸, Alice M. Grimm⁹, Kyung-Ja Ha^{10,11,12}, Harry Hendon¹³, Akio Kitoh^{14,15}, R.5 Krishnan¹⁶, June-Yi Lee^{11,12}, Jianping Li^{17,18}, Jian Liu¹⁹, Aurel Moise²⁰, Salvatore Pascale²¹, M. K.6 Roxy¹⁶, Anji Seth²², Chung-Hsiung Sui⁶, Andrew Turner^{23,24}, Song Yang^{25,26}, Kyung-Sook Yun¹¹,7 Lixia Zhang²⁷, Tianjun Zhou²⁷

8

9 ¹ Department of Atmospheric Sciences, University of Hawaii, Honolulu, HI, USA10 ² Lamont-Doherty Earth Observatory, Columbia University, Palisades, NY, USA11 ³ School of Earth & Environmental Sciences, University of St Andrews, St. Andrews, UK12 ⁴ Department of Physics, University of Oxford, Oxford, UK13 ⁴ Department of Hydrology and Atmospheric Sciences, University of Arizona, Tucson, AZ, USA14 ⁵ Department of Meteorology, Naval Postgraduate School, Monterey, CA, USA15 ⁶ Department of Atmospheric Sciences, National Taiwan University, Taipei, Taiwan16 ⁷ Department of Geological Sciences, University of Texas, Austin, TX, USA17 ⁸ Department of Atmospheric and Oceanic Sciences, University of California, Los Angeles, CA,

18 USA

19 ⁹ Department of Physics, Federal University of Paraná, Curitiba, Brazil20 ¹⁰ Department of Atmospheric Sciences, Pusan National University, Busan, Republic of Korea21 ¹¹ Institute for Basic Science, Center for Climate Physics, Busan, Republic of Korea22 ¹² Research Center for Climate Sciences and Department of Climate System, Pusan National

23 University, Busan, Republic of Korea

24 ¹³ Bureau of Meteorology, Melbourne, Australia

25 ¹⁴ Japan Meteorological Business Support Center, Tsukuba, Japan

26 ¹⁵ Meteorological Research Institute, Tsukuba, Japan

27 ¹⁶ Indian Institute of Tropical Meteorology, Pune, India

28 ¹⁷ Institute for Advanced Ocean Studies, Ocean University of China, Qingdao, China

29 ¹⁸ Pilot Qingdao National Laboratory for Marine Science and Technology, China

30 ¹⁹ School of Geographic and Oceanographic Sciences, Nanjing Normal University, Nanjing, China

31 ²⁰ Center for Climate Research Singapore, Republic of Singapore

32 ²¹ Department of Earth System Sciences, Stanford University, Stanford, CA, USA

33 ²² Department of Geography, University of Connecticut, Storrs, CT, USA

34 ²³ Department of Meteorology, University of Reading, Reading, UK

35 ²⁴ National Centre for Atmospheric Science, University of Reading, Reading, UK

36 ²⁵ School of Atmospheric Sciences and Guangdong Province Key Laboratory for Climate Change
37 and Natural Disaster Studies, Sun Yat-sen University, Guangzhou, China

38 ²⁶ Southern Marine Science and Engineering Guangdong Laboratory (Zhuhai), China

39 ²⁷ Institute of Atmospheric Physics, Chinese Academy of Sciences, China

40

41

42

43 Corresponding Author: Dr. Chih-Pei Chang, email:cpchang@nps.edu

44

45

46

Abstract

47 Monsoon rainfall has profound economic and societal impacts for more than two-thirds of the
48 global population. Here we provide a review on past monsoon changes and their primary
49 drivers, the projected future changes and key physical processes, and discuss challenges of the
50 present and future modeling and outlooks. Continued global warming and urbanization over
51 the past century has already caused a significant rise in the intensity and frequency of extreme
52 rainfall events in all monsoon regions (high confidence). Observed changes in the mean
53 monsoon rainfall vary by region with significant decadal variations. NH land monsoon rainfall as
54 a whole declined from 1950 to 1980 and rebounded after the 1980s, due to the competing
55 influences of internal climate variability and radiative forcing from GHGs and aerosol forcing
56 (high confidence); however, it remains a challenge to quantify their relative contributions.

57 The CMIP6 models simulate better global monsoon intensity and precipitation over CMIP5
58 models, but common biases and large intermodal spreads persist. Nevertheless, there is high
59 confidence that the frequency and intensity of monsoon extreme rainfall events will increase,
60 alongside an increasing risk of drought over some regions. Also, land monsoon rainfall will
61 increase in South Asia and East Asia (high confidence) and northern Africa (medium confidence),
62 and decrease in North America and unchanged in Southern Hemisphere. Over Asian-Australian
63 monsoon region the rainfall variability is projected to increase on daily to decadal scales. The
64 rainy season will likely be lengthened in the Northern Hemisphere due to late retreat
65 (especially over East Asia), but shortened in the Southern Hemisphere due to delayed onset.

66

67

68 Capsule Summary

69 This paper reviews the current knowledge on detection, attribution and projection of global
70 and regional monsoons (South Asian, East Asian, Australian, South American, North American,
71 and African) under climate change.

72

73 **1. Introduction**

74 Many parts of the Earth's surface and two-thirds of the global population are influenced
75 by the monsoon. This paper reviews the current state of knowledge of climate change and its
76 impacts on the global monsoon and its regional components, including recent results from
77 phase six of the Coupled Model Intercomparison Project (CMIP6) that were reported at a World
78 Meteorological Organization/World Weather Research Programme workshop held in Zhuhai in
79 early December 2019. The review's primary focus is on monsoon rainfall, both mean and
80 extremes, whose variability has tremendous economic and societal impacts. Due to the large
81 body of literature on this broad topic, only a fraction can be cited in this concise review.

82 The global monsoon (GM) is a defining feature of the Earth's climate and a forced
83 response of the coupled climate system to the annual cycle of solar insolation. For clarity, we
84 define the monsoon domain primarily based on rainfall contrast in the solstice seasons (Fig. 1).
85 The North American monsoon (NAM) domain covers western Mexico and Arizona, but also
86 Central America and Venezuela, and is larger than that traditionally recognized by many
87 scientists working on the NAM. We aim to encompass the range of literature marrying together
88 global monsoon, regional monsoon and paleoclimate monsoon perspectives and therefore
89 reach a compromise. Equatorial Africa and the Maritime Continent also feature annual reversal
90 of surface winds, although the former has a double peak in the equinoctial seasons and the
91 latter is heavily influenced by complex terrain (Chang 2004).

92 Our goal is to outline past changes of the monsoon and identify the key drivers of these
93 changes, assess the roles and impacts of natural and anthropogenic forcings and regional
94 variability, and discuss the limitations and difficulties of current climate models in representing

95 monsoon variability. We will also attempt to summarize projected future changes both globally
96 and in various monsoon regions using recent model results. Due to the inherent uncertainties
97 and model limitations, the degree of confidence in the results varies. A section on model issues
98 and outlook is devoted to discussing challenges of present and future monsoon modeling.

99 **2. Global monsoon**

100 2.1. Detection and Attribution of observed changes

101 Wang and Ding (2006) found a decreasing trend of global land monsoon precipitation
102 from the 1950s to 1980, mainly due to the declining monsoon in the northern hemisphere (NH).
103 After 1980, GM precipitation (GMP) has intensified due to a significant upward trend in the NH
104 summer monsoon (Wang et al., 2012). Extended analysis of the whole 20th century NH land
105 monsoon rainfall indicates that short-period trends may be part of multidecadal variability,
106 which is primarily driven by forcing from the Atlantic (Atlantic Multidecadal Variation; AMV,
107 and the Pacific (Interdecadal Pacific Oscillation; IPO) (Zhou et al. 2008, Wang et al. 2013, 2018;
108 Huang et al. 2020a). On the other hand, there is evidence that anthropogenic aerosols have
109 influenced decreases of NH land monsoon precipitation in the Sahel, South and East Asia during
110 the second half of the 20th century (Polson et al., 2014; Giannini and Kaplan, 2019; Zhou et al.,
111 2020b). It should be noted that this long-term decrease in precipitation could be, in part, due to
112 natural multi-decadal variations of the regional monsoon precipitation (Sontakke et al. 2008, Jin
113 and Wang 2017; Huang et al., 2020b). It remains a major challenge, however, to quantify the
114 relative contributions of internal modes of variability versus anthropogenic forcing on the
115 global scale.

116 2.2. Projected long-term changes

117 The CMIP5 results suggest that GM area, annual range and mean precipitation are likely
118 to increase by the end of the 21st century (Kitoh et al., 2013; Hsu et al., 2013; Christensen et al.,
119 2013). The increase will be stronger in the NH, and the NH rainy season is likely to lengthen due
120 to earlier or unchanged onset dates and a delayed retreat (Lee and Wang, 2014). The increase
121 in GM precipitation was primarily attributed to temperature-driven increases in specific
122 humidity, resulting in the “wet-get-wetter” pattern (Held and Soden, 2006).

123 Analysis of 34 CMIP6 models indicates a larger increase in monsoon rainfall over land
124 than over ocean in all four core Shared Socio-economic Pathways (SSPs) (Fig. 2; Lee et al. 2019).
125 The projected GMP increase over land by the end of the 21st century relative to 1995-2014 in
126 CMIP6 is about 50% larger than in CMIP5. Models with high (>4.2°C) equilibrium climate
127 sensitivity (ECS) account for this larger projection. The causes of CMIP6 models’ high ECS has
128 been discussed in Zelinka et al. (2020). Note that the forced signal of GMP over land shows a
129 decreasing trend from 1950 to the 1980s, but the trend reversed around 1990, which is
130 consistent with the CMIP5 results (Lee and Wang, 2014). During 1950-1990, the temperature-
131 driven intensification of precipitation was likely masked by a fast precipitation response to
132 anthropogenic sulfate and volcanic forcing, even though the warming trend due to GHG since
133 the pre-industrial period (1850-1900) is three times larger than the cooling due to aerosol
134 forcing (Lau and Kim, 2017; Richardson et al. 2018;). The recent upward trend may signify the
135 emergence of the greenhouse-gas signal against the rainfall reduction due to aerosol emissions.
136 However, the trend during recent decades can be influenced by the leading modes of
137 multidecadal variability of global SST (Wang et al. 2018). Lee et al. (2019) found that land
138 monsoon precipitation sensitivity (precipitation change per degree of global warming) slightly

139 increases with the level of GHG forcing, whereas the ocean monsoon precipitation has almost
140 no sensitivity (Fig. 2). The GM land precipitation sensitivity has a median of 0.8 %/°C in SSP2-4.5,
141 and a median of 1.4%/°C in SSP5-8.5. The latter is slightly higher than that simulated by CMIP5
142 models under RCP 8.5.

143 Wang et al. (2020) examined the ensemble-mean projection from 15 early-released
144 CMIP6 models, which estimates that under SSP2-4.5 the total NH land monsoon precipitation
145 will increase by about 2.8%/°C in contrast to little change in the southern hemisphere (SH; -
146 0.3%/°C). In both hemispheres, the annual range of land monsoon rainfall will increase by
147 about 2.6%/°C, with wetter summers and drier winters. In addition, the projected land
148 monsoon rainy season will be lengthened in the NH (by about ten days) due to late retreat, but
149 will be shortened in the SH due to delayed onset; the interannual variations of GMP will be
150 more strongly controlled by ENSO variability (Wang et al. 2020). In monsoon regions, increases
151 in specific humidity are spatially uniform (Fig. 4b), but the rainfall change features a robust NH-
152 SH asymmetry and an east-west asymmetry between enhanced Asian-African monsoons and
153 weakened NAM (Fig. 4a), suggesting that circulation changes play a crucial role in shaping the
154 spatial patterns and intensity of GM rainfall changes (Wang et al. 2020). GHG-induced
155 horizontally differential heating results in a robust “NH-warmer-than-SH” pattern (Fig. 4c),
156 which enhances NH monsoon rainfall (Liu et al. 2009, Mohtadi et al. 2016), especially in Asia
157 and northern Africa, due to an enhanced thermal contrast between the large Eurasia-Africa
158 landmass and adjacent oceans (Endo et al. 2018). Those CMIP models that project a stronger
159 inter-hemispheric thermal contrast generate stronger Hadley circulations, more northward
160 positions of the ITCZ, and enhanced NH monsoon precipitation (Wang et al. 2020). The GHG

161 forcing also induces a warmer equatorial eastern Pacific (Fig. 4c), which reduces NAM rainfall by
162 shifting the ITCZ equatorward (Wang et al. 2020). Climate models on average predict
163 weakening ascent under global warming (Endo and Kitoh, 2014), which tends to dry monsoon
164 regions. Weakening monsoon ascent has been linked to the slowdown of the global overturning
165 circulation (Held and Soden 2006). However, a definitive theory for why monsoon circulations
166 broadly weaken with warming remains elusive.

167 Land monsoon rainfall (LMR) provides water resources for billions of people; an
168 accurate prediction of its change is vital for the sustainable future of the planet. Regional land
169 monsoon rainfall exhibits very different sensitivities to climate change (Fig. 3). The annual mean
170 LMR in the East Asian and South Asian monsoons shows large positive sensitivities with means
171 of 4.6%/°C, and 3.9%/°C, respectively, under SSP2-4.5. The LMR likely increases in NAF, but
172 decreases in NAM, and remains unchanged in the Southern Hemisphere monsoons (Jin et al.
173 2020).

174 2.3. Projected near-term change

175 The interplay between internal modes of variability, such as IPO, AMV and SH Annular
176 Mode (Zheng et al. 2014), and anthropogenic forcing is important in the historical record and
177 for the near-term future (Chang et al. 2014). Huang et al. (2020a) used two sets of initial
178 condition large ensembles to suggest that internal variability linked to the IPO could overcome
179 the forced upward trend in the South Asian monsoon rainfall up to 2045. Using 20th-century
180 observations and numerical experiments, Wang et al. (2018) showed that the hemispheric
181 thermal contrast in the Atlantic and Indian Oceans and the IPO can be used to predict the NH
182 land monsoon rainfall change a decade in advance. The significant decadal variability of

183 monsoon rainfall leads to considerable uncertainties in climate projections for the next 30 years;
184 thus, improvements in predicting internal modes of variability could reduce uncertainties in
185 near-term climate projections.

186 **3. Regional monsoon changes**

187 3.1 South Asian monsoon

188 The South Asian summer monsoon (SASM) circulation experienced a significant
189 declining trend from the 1950s together with a weakening local meridional circulation and
190 notable precipitation decreases over north-central India and the west coast that are associated
191 with a reduced meridional temperature gradient (e.g., Krishnan et al., 2013, Roxy et al. 2015).
192 This trend was attributed to effects of anthropogenic aerosol forcing (e.g., Salzmänn et al., 2014;
193 Krishnan et al. 2016) and equatorial Indian Ocean warming due to increased GHG (e.g.,
194 Sabeerali and Ajayamohan 2017). However, it could potentially be altered by multidecadal
195 variations (Shi et al. 2018) arising from internal modes of climate variability such as the IPO and
196 AMV (e.g., Krishnan and Sugi, 2003, Salzmänn and Cherian, 2015, Jiang and Zhou 2019). The
197 processes by which aerosols affect monsoons were reviewed by Li et al. (2015). Aerosols can
198 also have a remote impact on regional monsoons (Shaeki et al., 2018).

199 CMIP models consistently project increases in the mean and variability of SASM
200 precipitation, despite weakened circulation at the end of the 21st century relative to the
201 present (e.g., Kitoh et al. 2013; Wang et al. 2014), though some models disagree (Sabeerali and
202 Ajayamohan 2017). The uncertainty in radiative forcing from aerosol emissions in CMIP5 causes
203 a large spread in the response of SASM rainfall (Shonk et al., 2019). However, this is not the
204 case in CMIP6 projections (Fig. 3).

205 3.2 East Asian monsoon

206 During the 20th century, East Asian summer monsoon (EASM) exhibited considerable
207 multi-decadal variability with a weakened circulation and a south flood-north drought pattern
208 since the late 1970s (Zhou 2009; Ding et al. 2009). The south flood-north drought pattern has
209 been predominantly attributed to internal variability, especially the phase change of the IPO (Li
210 et al. 2010, Nigam et al 2015, Ha et al. 2020a), and aided by GHG-induced warming (Zhu et al.
211 2012), and increased Asian aerosols emissions from the 1970s to 2000s (Dong et al., 2019).
212 Since 1979, both sea-surface temperature (SST) and atmospheric heating over Southeast Asia
213 and adjacent seas have increased significantly (Li et al. 2016), which may have led to decreased
214 rainfall over East Asia, South Asia (Annamalai et al., 2013) and the Sahel region (He et al. 2017).

215 Analysis of 16 CMIP6 models indicates that, under the SSP2-4.5 scenario, EASM
216 precipitation will increase at 4.7 %/°C (Ha et al. 2020b), with dynamic effects more important
217 than thermodynamic effects (Oh et al., 2018; Li et al. 2019). EASM duration is projected to
218 lengthen by about five pentads due to earlier onset and delayed retreat (Ha et al. 2020b), which
219 is comparable to previous assessment results (Endo et al. 2012, Kitoh et al. 2013, Moon and Ha
220 2017).

221 3.3 African monsoon

222 West Africa rainfall totals in the Sahel have been increasing since the 1980s, which
223 helped greening (Taylor et al. 2017; Brandt et al. 2019). Much of the increase in seasonal
224 rainfall is owed to positive trends in mean intensity (Lodoun et al. 2013, Sarr et al. 2013),
225 rainfall extremes (Panthou et al. 2014, Sanogo et al. 2015), and the frequency of intense
226 mesoscale convective systems (Taylor et al. 2017). Several West African countries have

227 experienced trends towards a wetter late season and delayed cessation of the rains (Lodoun et
228 al. 2013, Brandt et al. 2019). All the above changes are qualitatively consistent with
229 the CMIP5 response to GHG (Marvel et al., 2019). Preliminary results from CMIP6
230 confirm that the Sahel will become wetter, except for the west coast, and the rainy season will
231 extend later (Supplementary Fig. S1). Yet, the range of simulated variability has not improved,
232 and large quantitative uncertainties in the projections persist. In spite of the large spread, the
233 CMIP6 models project that NAF land monsoon rainfall will likely increase (Fig. 3).

234 In East Africa, observed increases in the boreal fall short rains are more robust (e.g.,
235 Cattani et al. 2018) than negative trends in the spring long rains (e.g., Maidment et al. 2015).
236 Regionality is pronounced, and there is sensitivity to Indian Ocean SSTs and Pacific variability
237 (Liebmann et al. 2014; Omondi et al. 2013). Selected CMIP6 models project little agreement on
238 how East African rainfall will change (supplementary Fig. S2), while some regional models
239 suggest enhanced rainfall during the short rains and a curtailed long-rains season (Cook and
240 Vizy 2013; Han et al. 2019). In the Congo Basin, observed precipitation trends are inconclusive
241 (Zhou et al. 2014; Cook and Vizy 2019), but one study reports earlier onset of the spring rains
242 (Taylor et al. 2018). A preliminary analysis finds overall improvement in CMIP6 models in the
243 overestimation of Congo Basin rainfall, though projections of changes under the SSP2-4.5
244 scenario are inconsistent. (Supplementary Fig. S3).

245 The CMIP6 models project that under SSP2-4.5 scenario and by the latter part of 21st
246 century, the SAF land monsoon rainfall will likely increase in summer but considerably reduce in
247 winter, so that the annual range will amplify but the annual mean rainfall will not change
248 significantly (Fig. 3)

249 3.4 Australian monsoon

250 Observations show increasing trends in mean and extreme rainfall over northern,
251 especially northwestern Australia since the early 1970s (Dey et al. 2019). Although Australian
252 summer monsoon rainfall has exhibited strong decadal variations during the 20th and early 21st
253 century, making detection and attribution of trends challenging, the recent upward trend since
254 1970s has been attributed to direct thermal forcing by increasing SST in the tropical western
255 Pacific (Li et al. 2013) and to aerosol and GHG forcing (Rotstayn et al. 2007, Salzmann 2016).

256 Australian monsoon rainfall is projected to increase by an average of 0.4%/°C in 33
257 CMIP5 models (Dey et al. 2019), although there is a large spread in the magnitude and even the
258 direction of the projected change. By selecting the best performing models for the Australian
259 monsoon, Joudain et al. (2013) found that seven of ten “good” CMIP5 models indicate a 5-20%
260 increase in monsoon rainfall over northern (20°S) Australian land by the latter part of the
261 21st century, but trends over a much larger region of the Maritime Continent are more
262 uncertain. Narsey et al. (2019) found that the range in Australian monsoon projections from the
263 available CMIP6 ensemble is substantially reduced compared to CMIP5, however, models
264 continue to disagree on the magnitude and direction of change. The CMIP6 models project that
265 summer and annual mean LMR changes are insignificant under SSP2-4.5; but the winter LMR
266 will likely decrease (Fig. 3) due to the enhanced Asian summer monsoon. By the end of the 21st
267 century, the Madden-Julian Oscillation (MJO) is anticipated to have stronger amplitude rainfall
268 variability (Maloney et al. 2018), but the impact on Australian summer monsoon intraseasonal
269 variability is uncertain (Moise et al. 2019).

270 3.5 North American monsoon

271 Observed long-term 20th century rainfall trends are either negative or null, but the
272 trends can vary substantially within this region (Pascale et al., 2019). During the period of
273 1950-2010 the monsoonal ridge was strengthened and shifted the patterns of transient
274 inverted troughs making them less frequent in triggering severe weather (Lahmers et al., 2016).
275 Recent observational and modeling studies show an increase in the magnitude of extreme
276 events in NAM and Central American rainfall under anthropogenic global warming (Aguilar et
277 al., 2005; Luong et al., 2017).

278 Climate models suggest an early-to-late redistribution of the mean NAM precipitation
279 with no overall reduction (Seth 2013, Cook and Seager, 2013), and a more substantial reduction
280 for Central American precipitation (Colorado-Ruiz et al., 2019). However, there is low
281 confidence in these projections, since both local biases (the models' representation of
282 vegetation dynamics, land cover and use, soil moisture hydrology) and remote biases (current
283 and future SST) may lead to large uncertainties (Bukovsky et al., 2015; Pascale et al., 2017).
284 Confidence in mean precipitation changes is lower than in the projection that precipitation
285 extremes are likely to increase due to the changing thermodynamic environment (Luong et al.
286 2017; Prein et al., 2016).

287 Figure 5 schematically sums up the factors that are likely to be determinant in the future
288 behavior of the NAM: the expansion and northwestward shift of the NAM ridge, and the
289 strengthening of the remote stabilizing effect due to SST warming are shown, and more intense
290 MCS-type convection. More uncertain remains the future of the NAM moisture surges and the
291 track of the upper-level inverted troughs, which are key synoptic processes controlling
292 convective activity.

293 3.6 South American monsoon

294 A significant positive precipitation trend since the 1950s till the 1990s was observed in
295 southeast South America, and has been related to interdecadal variability (Grimm and Saboia,
296 2015), ozone depletion and increasing GHG (Gonzalez et al. 2014; Vera and Diaz 2015). The
297 trend in the tropical South American monsoon is less coherent due to the influence of the
298 tropical Atlantic and the tendency to reverse rainfall anomalies from spring to summer in the
299 central-east South America due to land-atmosphere interactions (Grimm et al. 2007). In recent
300 decades the dry season has been lengthened and become drier, especially over the southern
301 Amazonia, which has significant influences on vegetation and moisture transport to the SAM
302 core region (Fu et al. 2013).

303 The CMIP6 models-projected future precipitation changes resemble the anomalies
304 expected for El Niño: little change of total precipitation (Figs. 3 and 4). This is consistent with El
305 Niño impacts (Grimm 2011) and CMIP5 projections (Seth et al. 2013). CMIP5 also projected
306 reduction of early monsoon rainfall while peak season rainfall increases, a delay and shortening
307 of the monsoon season (Seth et al. 2013), and prolonged dry spells between the rainy events
308 (Christensen et al., 2013). However, inter-model discrepancies are large (Yin et al., 2013).
309 CMIP5 models also likely underestimate the climate variability of the South American monsoon
310 and its sensitivity to climate forcing (Fu et al., 2013). Bias-corrected projections generally show
311 a drier climate over eastern Amazonia (e.g., Duffy et al., 2015; Malhi et al., 2008). Thus, the risk
312 of strong climatic drying and potential rainforest die-back in the future remains real.

313 **4. Extreme precipitation events in summer monsoons**

314 4. 1. Past changes and attribution

315 Over the past century, significant increases in extreme precipitation in association with
316 global warming have emerged over the global land monsoon region as a whole, and annual
317 maximum daily rainfall has increased at the rate of about 10-14%/°C in the southern part of the
318 South African monsoon, about 8%/°C in the South Asian monsoon, 6-11%/°C in the NAM, and
319 15-25%/°C in the eastern part of the South American monsoon (Zhang and Zhou 2019). At Seoul,
320 Korea, one of the world's longest instrumental measurements of daily precipitation since 1778
321 shows that the annual maximum daily rainfall and the number of extremely wet days, defined
322 as the 99th percentile of daily precipitation distribution, all have an increasing trend significant
323 at the 99% confidence level (Fig. 6). In the central Indian subcontinent, a significant shift
324 towards heavier precipitation in shorter duration spells occurred from 1950–2015 (Fig. 7) (Roxy
325 et al. 2017, Singh et al. 2019). In East Asia, the average extreme rainfall trend increased from
326 1958 to 2010, with a decreasing trend in northern China that was offset by a much larger
327 increasing trend in southern China (Chang et al. 2012). Over tropical South America, extreme
328 indices such as annual total precipitation above the 99th percentile and the maximum number
329 of consecutive dry days display more significant and extensive trends (Skansi et al. 2013, Hilker
330 et al. 2014).

331 Attribution studies show that global warming has already increased the frequency of
332 heavy precipitation since the mid-20th Century. An optimal fingerprinting analysis shows that
333 anthropogenic forcing has made a detectable contribution to the observed shift towards heavy
334 precipitation in eastern China (Ma et al. 2017). Simulations with all and natural-only forcing
335 show that global warming increased the probability of the 2016 Yangtze River extreme summer
336 rainfall by 17%–59% (Yuan et al. 2018). A large ensemble experiment also showed that

337 historical global warming has increased July maximum daily precipitation in western Japan
338 (Kawase et al. 2019).

339 Another anthropogenic forcing is urbanization. A significant correlation between rapid
340 urbanization and increased extreme hourly rainfall has been detected in the Pearl River Delta
341 and Yangtze River Delta of coastal China (Fig. 8) (Wu et al. 2019, Jiang et al. 2019). The
342 increasing trends are larger in both extreme hourly rainfall and surface temperature at urban
343 stations than those at nearby rural stations. The correlation of urbanization and extreme
344 rainfall is due to the urban heat island effect, which increases instability and facilitates deep
345 convection. Large spatial variability in the trends of extreme rainfall in India due to urbanization
346 and changes in land-use and land-cover has also been detected (Ali and Mishra 2017).

347 Land-falling tropical cyclones (TCs) make large contributions to heavy precipitation in
348 coastal East Asia. In the last 50 years, the decreasing frequency of incoming western North
349 Pacific (WNP) TCs more than offsets the increasing TC rainfall intensity, resulting in reduced TC-
350 induced extreme rainfall in southern coastal China, so the actual increase in non-TC extreme
351 rainfall is even larger than observed (Chang et al. 2012). Evidence in the WNP, and declining TC
352 landfall in eastern Australia (Nicholls et al. 1998), suggest that this poleward movement reflects
353 greater poleward TC recurvature.

354 4.2. Future Projection

355 One of the most robust signals of projected future change is the increased occurrence of
356 heavy rainfall on daily-to-multiday time scales and intense rainfall on hourly time scales. Heavy
357 rainfall will increase at a much larger rate than the mean precipitation, especially in Asia (Kitoh,
358 2013, 2017). Unlike mean precipitation changes, heavy and intense rainfall is more tightly

359 controlled by the environmental moisture content related to the Clausius-Clapeyron
360 relationship and convective-scale circulation changes. On average, extreme five-day GM rainfall
361 responds approximately linearly to global temperature increase at a rate of 5.17 (4.14–
362 5.75)%/°C under RCP8.5 with a high signal-to-noise ratio (Zhang et al. 2018). Regionally,
363 extreme precipitation in the Asian monsoon region exhibits the highest sensitivity to warming,
364 while changes in the North American and Australian monsoon regions are moderate with low
365 signal-to-noise ratio (Zhang et al. 2018). CMIP6 models project changes of extreme 1-day
366 rainfall of +58% over South Asia and +68% over East Asia in 2065–2100 compared to 1979–2014
367 under the SSP2-4.5 scenario (Ha et al. 2020b). Model experiments also indicate a three-fold
368 increase in the frequency of rainfall extremes over the Indian subcontinent under future
369 projections for global warming of 1.5°C–2.5°C (Bhowmick et al. 2019). Meanwhile, light-to-
370 moderate rain events may become less frequent (Sooraj et al. 2016).

371 Changes in the variability of monsoon rainfall may occur on a range of time scales.
372 Brown et al. (2017) found increased rainfall variability under RCP8.5 for each time scale from
373 daily to decadal over the Australian, South Asian, and East Asian monsoon domains (Fig. 8). The
374 largest fractional increases in monsoon rainfall variability occur for South Asian at all sub-
375 annual time scales and for the East Asian monsoon at annual-to-decadal time scales. Future
376 changes in rainfall variability are significantly positively correlated with changes in mean wet
377 season rainfall for each of the monsoon domains and for most time scales.

378 Selected CMIP5 models project more severe floods and droughts in the future climate
379 over South Asia (Sharmila et al. 2015; Singh et al. 2019). Due to more rapidly rising evaporation,
380 the projections for 2015–2100 under CMIP6 SSP2-4.5 and SSP5-8.5 scenarios indicate that the

381 western part of East Asia will confront more rapidly increasing drought severity and risks than
382 the eastern part (Ha et al. 2020b).

383 Projections of future extreme rainfall change in the densely populated and fast-growing
384 coastal zones are particularly important for several reasons. First, in fast-growing urban areas,
385 extreme rainfall will likely intensify in the future, depending on the economic growth of the
386 affected areas. Second, future extreme rainfall changes in coastal areas will be affected by
387 future changes in landfalling TCs. For instance, TC projections (Knutson et al. 2019b) suggest a
388 continued (albeit with lower confidence) northward trend. Assuming this means more
389 recurvature cases, it would lead to extreme rainfall increases in coastal regions of Korea and
390 Japan and decreases in China. Third, the increase in monsoon extreme rains and TCs, together
391 with rising sea level will lead to aggravated impacts, for instance, along coastal regions of the
392 Indian subcontinent (Collins et al. 2019).

393 **5. Model Issues and Future Outlook**

394 5.1 Major common issues and missing processes

395 CMIP6 models improve the simulation of present-day solstice season precipitation
396 climatology and the GM precipitation domain and intensity over the CMIP5 models; and CMIP6
397 models reproduce well the annual cycle of the NH monsoon and the leading mode of GM
398 interannual variability and its relationship with ENSO (Wang et al. 2020). However, the models
399 have major common biases in equatorial oceanic rainfall and SH monsoon rainfall, including
400 overproduction of annual mean SH monsoon precipitation by more than 20%, and the
401 simulated onset is early by two pentads while the withdrawal is late by 4-5 pentads (Wang et al.
402 2020). Systematic model biases in monsoon climates have persisted through generations of

403 CMIP (e.g., Sperber et al., 2013). In particular, the poor representation of precipitation
404 climatology is seen in many regional monsoons, such as Africa (Creese and Washington 2016,
405 Han et al. 2019), and North America (Geil et al., 2013). These biases are often related to SST
406 biases in adjacent oceans (Cook and Vizy 2013, Pascale et al., 2017). There are additional
407 outstanding common issues for regional monsoon simulations, which are not immediately
408 apparent in quick-look analyses. A major one is the diurnal cycle, which is poorly simulated in
409 the tropics, due to failures in convective parameterization (Willettts et al., 2017). Biases in
410 evapotranspiration also affect the Bowen ratio (Yin et al. 2013), and thus atmospheric boundary
411 layer humidity and height. Biases in variability emerge in historical monsoon simulations,
412 hampering accurate attribution of present-day monsoon changes (Herman et al. 2019; Marvel
413 et al, 2019) and amplifying uncertainties in future projections.

414 While there are subtle improvements from CMIP3 to CMIP5 and to CMIP6 due to steady
415 increases in horizontal resolution and improved parameterizations, simulation of monsoon
416 rainfall is still hampered by missing or poorly resolved processes. These include the lack of
417 organized convection (e.g., mesoscale convective systems or monsoon depressions) at coarse
418 model resolutions, poorly simulated orographic processes, and imperfect land-atmosphere
419 coupling due to under-developed parametrizations and a paucity of observations of land-
420 atmosphere exchanges that can only be improved through field observation programs (e.g.
421 Turner et al., 2019). Further, proper simulation of how aerosols modify monsoon rainfall
422 requires improved cloud microphysics schemes (Yang et al., 2017; Chu et al., 2018). Finally,
423 some features of monsoon meteorology that are crucial to climate projection and adaptation,
424 such as extreme rainfall accumulations exceeding 1 meter/day, are nearly impossible to

425 simulate in coupled climate models. High-resolution regional simulations can potentially
426 ameliorate biases, but they still must rely on GCM-generated boundary conditions in their
427 projections. Convection-permitting regional simulations have been suggested to more
428 realistically represent short time scale rainfall processes and their responses to forcing (e.g. in
429 future simulations for Africa; Kendon et al., 2019).

430 5.2 Sources of model uncertainty in future projection of monsoons

431 The major sources of projection uncertainty include model uncertainty, scenario
432 uncertainty and internal variability. Contributions from internal variability decrease with time,
433 while those from scenario uncertainty increase. Model uncertainty dominates near-term
434 projections of GM mean and extreme precipitation with a contribution of ~90% (Zhou et al.
435 2020a). Model uncertainty often arises from divergent circulation changes. In particular,
436 circulation changes caused by regional SST warming and land-sea thermal contrast can
437 generally contribute to uncertainty in monsoon rainfall changes (Chen and Zhou, 2015; Pascale
438 et al., 2017). Uncertainty in projected surface warming patterns is closely related to present-
439 day model biases, including the cold-tongue bias in the tropical eastern Pacific (Chen and Zhou,
440 2015; Ying et al. 2019) and a cold bias beneath underestimated marine stratocumulus, which
441 can induce a large land-sea thermal contrast in the future (Nam et al. 2012, Chen et al. 2019).
442 Monsoons are strongly influenced by cloud and water vapor feedbacks (Jalihal et al., 2019;
443 Byrne and Zanna, 2020), yet how the large variations in these feedbacks across climate models
444 impact monsoon uncertainties is unknown. Another factor affecting future monsoon changes
445 are vegetation feedbacks. Cui et al. (2019) showed that they may exacerbate the effects of CO₂-
446 induced radiative forcing, especially in the North and South American and Australian monsoons

447 via reduced stomatal conductance and transpiration. Vegetation is an important water vapor
448 provider and can affect monsoon onsets (Wright et al. 2017; Sori et al. 2017), yet current
449 climate models have limited capability in representing how vegetation responds to climate and
450 elevated CO₂, and how land use and fires affect future vegetation distribution and functions.
451 The extent to which these model limitations contribute to the uncertainty of future monsoon
452 rainfall projections is virtually unknown, although plant physiological effects may exacerbate
453 CO₂-radiative impacts (Cui et al., 2019). While CMIP6 models are more advanced in terms of
454 physical processes included and resolution, the inter-model spread in projection of monsoons
455 in CMIP6 models has remained as large (or became larger) compared to CMIP5 models (Fig 2).

456 5.3 Future Outlook

457 Future models might improve by explicitly resolving deep convection to address
458 common problems across monsoon systems. In attribution, controversies remain over the
459 relative roles of natural multidecadal variability and anthropogenic forcing, especially of aerosol
460 effects on the observed historical monsoon evolution in Asia and West Africa. Quantification of
461 the roles of multidecadal variability in biasing the transient climate sensitivity in observations as
462 well as in model simulations is encouraged.

463 There is an urgent need to better understand sources of uncertainty in future rainfall
464 projections. Such sources encompass but are not limited to structural uncertainty, uncertainties
465 in aerosol processes and radiative forcing, the roles of internal modes of variability and their
466 potential changes in the future, ecosystem feedbacks to climate change and elevated CO₂, and
467 land-use impacts. To have more confidence in future projections, we need to quantify the
468 causes of spread in future climate signals at the process level: the relative magnitudes of

469 forcing uncertainty versus mean-state biases and feedback uncertainties. This type of error
470 quantification requires specially designed, coordinated simulations across modelling centers
471 and a focus on the key processes that need to be improved.

472 Traditional future assessments of the global monsoon continue to rely on multi-model
473 approaches. However, a small multi-model ensemble such as CMIP5 or CMIP6 may not
474 represent the full extent of uncertainty introduced by internal (multi-decadal) variability. More
475 recently, large ensembles are being employed to help understand the spread or degree of
476 uncertainty in a climate signal, and, at the regional level, the interplay between internal
477 variability and anthropogenic external forcing in determining a climate anomaly. Such large
478 ensembles are either perturbed-parameter ensembles (PPE) (Murphy et al., 2014) or
479 alternatively, traditional initial-condition ensembles – e.g., by CanESM2 (Sigmond and Fyfe,
480 2016; Kirchmeier-Young, 2017) or by MPI-ESM (Maher et al., 2019) – with tens to a hundred
481 members. Large-ensemble methods should be applied to the global monsoon in order to
482 determine the extent to which internal variability can explain its declining rainfall in the late
483 20th century. We suggest that an additional pathway to more reliable monsoon projections
484 would be to develop emergent constraints applicable to monsoons, and this should be a focus
485 for the research community.

486 Recent theoretical advances in tropical atmospheric dynamics offer new avenues to
487 further our understanding of monsoon circulations in a changing climate. Monsoon locations
488 have been shown to coincide with maxima in sub-cloud moist static energy (MSE) (Privé and
489 Plumb 2007), with MSE budgets likely to be useful for understanding the response of monsoons
490 to external forcing (Hill 2019). Recent studies of the ITCZ may also provide new insights into the

491 strength and spatial extent of monsoons. Theoretical work has identified energetic (Sobel and
492 Neelin, 2006; Byrne and Schneider, 2016) and dynamical constraints (Byrne and Thomas, 2019)
493 on the width of the ITCZ, with implications for its strength (Byrne et al., 2018). Additionally,
494 Singh et al. (2017) have linked the strength of the Hadley circulation to meridional gradients in
495 moist entropy. The extent to which these theories can explain CMIP6 changes in monsoon
496 strength and spatial extent is an open question that should be prioritized.

497 Understanding past monsoon responses to external forcings may shed light on future
498 climate change. The NH monsoon future response is shown to be weaker than in simulations of
499 the mid-Holocene, although future warming is larger (D'Agostino et al. 2019). This occurs
500 because both thermodynamic and dynamic responses act in concert and cross-equatorial
501 energy fluxes shift the ITCZ towards the warmer NH during the mid-Holocene, but in the future,
502 they partially cancel. The centennial-millennial variations of GM precipitation before the
503 industrial period are mainly attributable to solar and volcanic (SV) forcing (Liu et al., 2009). For
504 the same degree of warming, GHG forcing induces less rainfall increase than SV forcing because
505 the former increases stability, favoring a weakened Walker circulation and El Niño-like warming,
506 while the latter warms tropical Pacific SSTs in the west more than the east, favoring a La Nina-
507 like warming through the ocean thermostat mechanism (Liu et al. 2013). An El Niño-like
508 warming reduces GM precipitation (Wang et al. 2012). Jaliha et al. (2019), by examining
509 responses of tropical precipitation to orbital forcing, find that the changes in precipitation over
510 land are mainly driven by changes in insolation, but over the oceans, surface fluxes and vertical
511 stability play an important role in precipitation changes.

512 **6. Summary**

513 We have reviewed past monsoon changes and their primary drivers, summarized
514 projected future changes and key physical processes, and discussed challenges of the present
515 and future modeling and outlooks. In this section we will assign a level of confidence to the
516 main conclusions wherever feasible.

517 *1. Extreme rainfall events.*

518 Continued global warming over the past century has already caused a significant rise in
519 the intensity and frequency of extreme rainfall events in all monsoon regions (e.g., Figs. 6 and 7;
520 high confidence). Urbanization presents additional anthropogenic forcing that significantly
521 increases localized extreme rainfall events in areas of rapid economic growth due to the urban
522 heat island effect (Fig. 8, high confidence). This urban effect is expected to expand to more
523 locations with the growing economy, especially in Asia. There is some indication that TC tracks
524 in the western North Pacific have been shifting more towards the recurvature type. If this trend
525 continues, it may cause an increase in the ratio of TC-related extreme rainfall in Korea and
526 Japan versus China (low confidence).

527 Almost all future projections agree that the frequency and intensity of extreme rainfall
528 events will increase. The occurrence of heavy rainfall will increase on daily-to-multiday time
529 scale and intense rainfall on hourly time scales. The increased extreme rainfall is largely due to
530 an increase in available moisture supply and convective-scale circulation changes. Meanwhile,
531 models also project prolonged dry spells between the heavy rainy events, which, along with
532 enhanced evaporation and runoff of ground water during heavy rainfall, will lead to an
533 increased risk of droughts over many monsoon regions (high confidence). Notably, the

534 enhanced extreme rain events will *likely* contribute to compound events—where increasing
535 tropical cyclones, rising sea level, and changing land conditions—may aggravate the impact of
536 floods over the heavily populated coastal regions.

537 2. Mean monsoon rainfall and its variability

538 Observed changes in the mean monsoon rainfall vary by region with significant decadal
539 variations that have been related to internal modes of natural variability. Since the 1950s, NH
540 anthropogenic aerosols may be a significant driver in the Sahel drought and decline of monsoon
541 rainfall in South Asia (medium-high confidence). NH land monsoon rainfall as a whole declined
542 from 1950 to 1980 and rebounded after the 1980s, due to the competing influence of internal
543 climate variability, radiative forcing from GHGs and aerosol forcing (high confidence); however,
544 it remains a challenge to quantify their relative contributions. CMIP6 historical simulations
545 suggest that anthropogenic sulfate and volcanic forcing likely masked the effect of GHG forcing
546 and caused the downward trend from 1950 to 1990 (Fig. 2); however, the recent upward trend
547 may signify the emergence of the greenhouse-gas signal against the rainfall reduction due to
548 aerosol emissions (medium-high confidence).

549 CMIP6 models project a larger increase in monsoon rainfall over land than over ocean
550 (Fig. 2). Land monsoon rainfall will likely increase in the NH, but change little in the SH (Figs. 2
551 and 4). Regionally, land monsoon rainfall will increase in South Asia and East Asia (high
552 confidence), and northern Africa (medium confidence), but decrease over North American
553 monsoon region (high confidence) (Fig. 3). The projected mean rainfall changes (either neutral
554 or slightly decreasing) over SH (American, Australian, and Southern African) monsoons have low

555 confidence due to a large spread. The future change of GM precipitation pattern and intensity
556 is determined by increased specific humidity and circulation changes forced by the vertically
557 and horizontally inhomogeneous heating induced by GHG radiative forcing. Under GHGs-
558 induced warming, the land monsoon rainy season changes considerably from region to region;
559 yet, as a whole, the rainy season will likely be lengthened in the NH due to late retreat (with
560 most significant change over East Asia), but shortened in the SH due to delayed onset. The
561 variability of monsoon rainfall is projected to increase on daily to decadal time scales over the
562 Asian-Australian monsoon region (Fig. 9). Models generally underestimate the magnitude of
563 observed precipitation changes, which poses a major challenge for quantitative attributions of
564 regional monsoon changes. The range of projected change of annual-mean global land
565 monsoon precipitation by the end of the 21st century in CMIP6 is *likely* about 50% larger than in
566 corresponding scenarios of CMIP5.

567

568 Acknowledgments

569 This work is a task of the World Meteorological Organization's (WMO) World Weather Research
570 Programme (WWRP). All authors are invited experts by the WMO/WWRP Working Group for
571 Tropical Meteorology Research. We wish to thank Sun Yat-sen University for hosting the WMO
572 Workshop on Monsoon Climate Change Assessment in Zhuhai, China, in which this review was
573 discussed. This work was supported in part by the National Natural Science Foundation of China
574 under Grant 91637208 to Sun Yat-sen University, and the following agencies and Grant/Project
575 numbers for individual coauthors: NSF 1612904 (Biasutti), 1701520 (Cook), 1917781 (Fu),
576 1540783 (Wang) ,1128040 (Grimm); Institute for Basic Science IBS-R028-D1 (Ha, Lee and Yun);
577 National Natural Science Foundation of China 41420104002 and 41971108 (Liu), 41675076
578 (Zhang); International Partnership Program of Chinese Academy of Sciences
579 134111KYSB20160031 (Zhou); MOST 108-2119-M-002-022 (Chang), 106-2111-M-002-003-001-
580 MY2 (Sui and Chang), 108-2111-M-002-016- (Sui); Ministry of Earth Sciences, Govt. of India
581 (Krishnan and Roxy); MEXT Integrated Research Program for Advancing Climate Models
582 JPMXD0717935457 (Kitoh); NERC NE/N018591/1 and NE/S004890/1 (Turner); U.S.
583 Departments of Defense and Energy and the U.S. Environmental Protection Agency Strategic
584 Environmental Research and Development Program RC-2205 (Castro); National Council for
585 Scientific and Technological Development and Inter-American Institute for Global Change
586 Research CRN3035 (Grimm).

587

588

589 **References**

- 590 Abbs, D., 2012: The impact of climate change on the climatology of tropical cyclones in the
591 Australian region. *Aspendale: CSIRO*, **11**, doi:10.4225/08/584ee7d4585f5.
- 592 Aguilar, E., T. C. Peterson, P. Ramírez Obando, R. Frutos, J. A. Retana, M. Solera, J. Soley, I.
593 González García, R. M. Araujo, A. Rosa Santos, V. E. Valle, M. Brunet, L. Aguilar, L.
594 Álvarez, M. Bautista, C. Castañón, L. Herrera, E. Ruano, J. J. Sinay, E. Sánchez, G. I.
595 Hernández Oviedo, F. Obed, J. E. Salgado, J. L. Vázquez, M. Baca, M. Gutiérrez, C.
596 Centella, J. Espinosa, D. Martínez, B. Olmedo, C. E. Ojeda Espinoza, R. Núñez, M.
597 Haylock, H. Benavides, and R. Mayorga 2005: Changes in precipitation and temperature
598 extremes in Central America and northern South America, 1961–2003. *J. Geophys. Res.*,
599 **110**, D23107.
- 600 Ali, H., and V. Mishra, 2017: Contrasting response of rainfall extremes to increase in surface air
601 and dewpoint temperatures at urban locations in India. *Scientific Reports*, **7**, 1228.
- 602 Annamalai, H., J. Hafner, K. P. Sooraj and P. Pillai, 2013: Global warming shifts the monsoon
603 circulation, drying South Asia. *J. Climate*, **26**, 2701-2718.
- 604 Bayr, T., D. Dommenges, T. Martin, and S. B. Power, 2014: The eastward shift of the Walker
605 circulation in response to global warming and its relationship to ENSO variability.
606 *Climate Dyn.*, **43**, 2747–2763, doi:10.1007/s00382-014-2091-y.
- 607 Bhowmick, M., S. Sahany, and S. K. Mishra, 2019: Projected precipitation changes over the
608 south Asian region for every 0.5° C increase in global warming. *Environ. Res. Lett.*, **14**,
609 054005, doi:10.1088/1748-9326/ab1271.

610 Bollasina, M. A., Y. Ming, and V. Ramaswamy, 2011: Anthropogenic aerosols and the weakening
611 of the South Asian summer monsoon. *Science*, **334**, 502-505.

612 Byrne, M. P., and T. Schneider, 2016: Narrowing of the ITCZ in a warming climate: physical
613 mechanisms. *Geophys. Res. Lett.*, **43**, 350.

614 Byrne, M. P., A. G. Pendergrass, A. D. Rapp, and K. R. Wodzicki, 2018: Response of the
615 intertropical convergence zone to climate change: Location, width, and strength.
616 *Current Climate Change Reports*, **4**, 355–370, doi:10.1007/s40641-018-0110-5.

617 Byrne, M. P., and R. Thomas, 2019: Dynamics of ITCZ width: Ekman processes, non-Ekman
618 processes, and links to sea surface temperature. *J. Atmos. Sci.*, **76**, 2869–2884.

619 Byrne, M. P., and L. Zanna, 2020: Radiative effects of clouds and water vapor on the monsoon.
620 *J. Climate*, in revision (preprint available at
621 https://drive.google.com/file/d/1HJgscJIqFR_tFFVHB-NxoyzJdQjJk4J/view).

622 Bukovsky, M. S., C. M. Carrillo, D. J. Gochis, D. M. Hammerling, R. R. McCrary, and L. O. Mearns,
623 2015: Toward assessing NARCCAP Regional Climate Model credibility for the North
624 American Monsoon: future climate simulations. *J. Climate*, **28**, 6707–6728.

625 Cai, W., X.-T. Zheng, E. Weller, M. Collins, T. Cowan, M. Lengaigne, T. Yamagata, 2013: Projected
626 response of the Indian Ocean dipole to greenhouse warming. *Nature Geoscience*, **6**,
627 999–1007.

628 Cai, W., G. Wang, A. Santoso, M. J. McPhaden, L. Wu, F.-F. Jin, and E. Guilyardi, 2015: Increased
629 frequency of extreme La Niña events under greenhouse warming. *Nature Climate
630 Change*, **5**, 132–137.

631 Cattani, E., A. Merino, J. A. Guijarro, and V. Levizzani, 2018: East Africa rainfall trends and
632 variability 1983–2015 using three long-term satellite products. *Remote Sensing*, **10**, 931,
633 doi:10.3390/rs10060931.

634 Chang, C. W. J., W.-L. Tseng, H.-H. Hsu, N. Keenlyside, and B.-J. Tsuang, 2015: The Madden-
635 Julian oscillation in a warmer world. *Geophys. Res. Lett.*, **42**, 6034–6042.

636 Chang, C.-P., M. Ghil, H.C. Kuo, M. Latif, C. H. Sui, and J. M. Wallace, 2014: Understanding
637 multidecadal climate changes. *Bull. Am. Meteorol. Soc.*, **95**, 293–296. doi:
638 10.1175/BAMS-D-13-00015.1.

639 Chang, C.-P., Y. Lei, C.-H. Sui, X. Lin, and F. Ren, 2012: Tropical cyclone and extreme rainfall
640 trends in East Asian summer monsoon since mid-20th century, *Geophys. Res. Lett.*, **39**,
641 L18702, doi:10.1029/2012GL052945.

642 Chang, C.-P., Z. Wang, J. McBride and C. H. Liu, 2005: Annual cycle of Southeast Asia - Maritime
643 Continent rainfall and the asymmetric monsoon transition. *J. Climate*, **18**, 287-301.

644 Chen, X., and T. Zhou, 2015: Distinct effects of global mean warming and regional sea surface
645 warming pattern on projected uncertainty in the South Asian summer monsoon.
646 *Geophys. Res. Lett.*, **42**, 9433–9439.

647 Chen, X., T. Zhou, P. Wu, Z. Guo, and M. Wang, 2019: Emergent constraints on future
648 projections of the western North Pacific Subtropical High. *Nat. Commun.*, under review.
649 Manuscript is available at [https://drive.google.com/open?id=1hkuL4G_xQ-](https://drive.google.com/open?id=1hkuL4G_xQ-2B6PBYGSMHXDhBrcAARaPZ)
650 [2B6PBYGSMHXDhBrcAARaPZ](https://drive.google.com/open?id=1hkuL4G_xQ-2B6PBYGSMHXDhBrcAARaPZ)

651 Christensen, J.H., K. Krishna Kumar, E. Aldrian, S.-I. An, I.F.A. Cavalcanti, M. de Castro, W. Dong,
652 P. Goswami, A. Hall, J.K. Kanyanga, A. Kitoh, J. Kossin, N.-C. Lau, J. Renwick, D.B.

653 Stephenson, S.-P. Xie and T. Zhou, 2013: Climate Phenomena and their Relevance for
654 Future Regional Climate Change. In: Climate Change 2013: The Physical Science Basis.
655 Contribution of Working Group I to the Fifth Assessment Report of the
656 Intergovernmental Panel on Climate Change [Stocker, T.F., D. Qin, G.-K. Plattner, M.
657 Tignor, S.K. Allen, J. Boschung, A. Nauels, Y. Xia, V. Bex and P.M. Midgley (eds.)].
658 Cambridge University Press, Cambridge, United Kingdom and New York, NY, USA.

659 Chu, J.-E., K.-M. Kim, W. K. M. Lau and K.-J. Ha, 2018: How light absorbing properties of organic
660 aerosol modify the Asian summer monsoon rainfall? *J. Geophys. Res. Atmos.*, **123**, 2244–
661 2255, doi:10.1002/2017JD027642.

662 Collins, M., and Coauthors, 2019: Extremes, Abrupt Changes and Managing Risk, in Portner et
663 al., eds. IPCC Special Report on Oceans and Cryosphere in a Changing Climate.
664 Cambridge University Press, Cambridge, United Kingdom and New York, NY, USA.

665 Cook, B. I. and R. Seager, 2013: The response of the North American Monsoon to increased
666 greenhouse gas forcing. *J. Geophys. Res.*, **118**, 1690–1699.

667 Cook, K. H., and E. K. Vizy, 2013: Projected changes in East African rainy seasons. *J. Climate*, **26**,
668 5931–5948, doi:10.1175/JCLI-D-12-00455.1

669 Cook, K. H., and E. K. Vizy, 2019: Congo Basin drying associated with poleward shifts of African
670 thermal lows. *Climate Dyn.*, doi:10.1007/s00382-019-05033-3.

671 Creese, A., and R. Washington, 2016: Using qflux to constrain modeled Congo Basin rainfall in
672 the CMIP5 ensemble. *J. Geophys. Res.*, **121**, 13415–13442, doi:10.1002/2016JD025596.

673 Cui, J., S. Piao, C. Huntingford, X. Wang, X. Lian, A. Chevuturi, A. G. Turner and G. J. Kooperman,
674 2019: Vegetation forcing modulates global land monsoon and water resources in a CO₂-

675 enriched climate. *Nature Geosciences*, submitted. The latest version of this paper is
676 available at: [https://livereadingac-](https://livereadingac-my.sharepoint.com/:f/g/personal/a_g_turner_reading_ac_uk/E18hjGgHjs5KooEbLEP0IIIBGgSajLlwumjN9ARCV7IJNQ?e=GrH4NI)
677 [my.sharepoint.com/:f/g/personal/a_g_turner_reading_ac_uk/](https://livereadingac-my.sharepoint.com/:f/g/personal/a_g_turner_reading_ac_uk/E18hjGgHjs5KooEbLEP0IIIBGgSajLlwumjN9ARCV7IJNQ?e=GrH4NI)
678 [E18hjGgHjs5KooEbLEP0IIIBGgSajLlwumjN9ARCV7IJNQ?e=GrH4NI](https://livereadingac-my.sharepoint.com/:f/g/personal/a_g_turner_reading_ac_uk/E18hjGgHjs5KooEbLEP0IIIBGgSajLlwumjN9ARCV7IJNQ?e=GrH4NI)

679 D'Agostino, R., J. Bader, S. Bordoni, D. Ferreira, and J. Jungclaus, 2019: Northern Hemisphere
680 monsoon response to mid-Holocene orbital forcing and greenhouse gas-induced global
681 warming. *Geophys. Res. Letts.*, **46**, 1591–1601, doi:10.1029/2018GL081589.

682 Deser, C., A. S. Phillips, and M. A. Alexander, 2010: Twentieth century tropical sea surface
683 temperature trends revisited. *Geophys. Res. Lett.*, **37**, L10701.

684 Dey, R., S. C. Lewis, J. M. Arblaster, and N. J. Abram, 2019: A review of past and projected
685 changes in Australia's rainfall. *Wiley Interdiscip. Rev. Clim. Chang.*, **10**, 1–23,
686 doi:10.1002/wcc.577.

687 Ding, Y., Y. Sun, Z. Wang, Y. Zhu, and Y. Song, 2009: Inter-decadal variation of the summer
688 precipitation in China and its association with decreasing Asian summer monsoon Part
689 II: Possible causes, *Int. J. Climatology*, **29**, 1926–1944.

690 Dong, B., L. J. Wilcox, E. J. Highwood, and R. T. Sutton, 2019: Impacts of recent decadal changes
691 in Asian aerosols on the East Asian summer monsoon: roles of aerosol–radiation and
692 aerosol–cloud interactions. *Climate Dyn.*, **53**, 3235, doi:10.1007/s00382-019-04698-0.

693 Duffy, P. B., P. Brando, G. P. Asner, and C. B. Field, 2015: Projections of future meteorological
694 drought and wet periods in the Amazon. *Proc. Natl. Acad. Sci. USA*, **112**, 13172–13177,
695 doi:10.1073/pnas.1421010112.

696 Endo, H., A. Kitoh, T. Ose, R. Mizuta, and S. Kusunoki, 2012: Future changes and uncertainties in
697 Asian precipitation simulated by multiphysics and multi-sea surface temperature
698 ensemble experiments with high-resolution Meteorological Research Institute
699 atmospheric general circulation models (MRI-AGCMs). *J. Geophys. Res.*, **117**, D16118,
700 doi:10.1029/2012JD017874.

701 Endo, H., and A. Kitoh, 2014: Thermodynamic and dynamic effects on regional monsoon rainfall
702 changes in a warmer climate. *Geophys. Res. Lett.*, **41**, 1704–1711.

703 Endo, H., A. Kitoh, and H. Ueda, 2018: A unique feature of the Asian summer monsoon
704 response to global warming: the role of different land–sea thermal contrast change
705 between the lower and upper troposphere. *SOLA*, **14**, 57–63, doi:10.2151/sola.2018-
706 010.

707 Fu, R., L. Yin, W. Li, P. A. Arias, R. E. Dickinson, L. Huang, S. Chakraborty, K. Fernandes, B.
708 Liebmann, R. Fisher, and R. B. Myneni, 2013: Increased dry-season length over southern
709 Amazonia in recent decades and its implication for future climate projection. *Proc. Natl.*
710 *Acad. Sci. USA*, **110**, 18110–18115, doi:10.1073/pnas.1302584110.

711 Geil, K. L., Y. L. Serra, and X. Zeng, 2013: Assessment of CMIP5 Model Simulations of the North
712 American Monsoon System. *J. Climate*, **26**, 8787–8801, doi:10.1175/JCLI-D-13-00044.1.

713 Giannini, A, and A. Kaplan, 2019: The role of aerosols and greenhouse gases in Sahel drought
714 and recovery. *Climatic Change*, **152**, 449-466.

715 Gonzalez, P. L. M., L. M. Polvani, R. Seager, G. J. Correa, 2014: Stratospheric ozone depletion: a
716 key driver of recent precipitation trends in South Eastern South America. *Climate Dyn.*,
717 **42**, 1775–1792.

718 Goswami, B. N., V. Venugopal, D. Sengupta, M. Madhusoodanan, and P. K. Xavier, 2006:
719 Increasing trend of extreme rain events over India in a warming environment. *Science*,
720 **314**, 1442–1445.

721 Grimm, A. M., J. Pal, and F. Giorgi, 2007: Connection between spring conditions and peak
722 summer monsoon rainfall in South America: Role of soil moisture, surface temperature,
723 and topography in eastern Brazil. *J. Climate*, **20**, 5929-5945.

724 Grimm, A. M., 2011: Interannual climate variability in South America: impacts on seasonal
725 precipitation, extreme events and possible effects of climate change. *Stochastic*
726 *Environmental Research and Risk Assessment*, 25, 537-554, DOI: 10.1007/s00477-010-
727 0420-1

728 Grimm, A. M., and J. P. J. Saboia, 2015: Interdecadal variability of the South American
729 precipitation in the monsoon season. *J. Climate*, **28**, 755-775, doi:10.1175/JCLI-D-14-
730 00046.1.

731 Ha, K. J., B. H. Kim, E. S. Chung, J. C. L. Chan, and C. P. Chang, 2020a: Major factors of monsoon
732 rainfall changes:natural versus anthropogenic forcing. *Environ. Res. Lett.*, doi:10.1088
733 /1748-9326/ab7767.

734 Ha, K. J., S. Moon, D. Kim, A. Timmermann, and D. Kim, 2020b: Future changes of summer
735 monsoon characteristics and evaporative demand over Asia in CMIP6 simulations.
736 *Geophys. Res. Lett.*, doi:10.1029/2020GL087492.

737 Han, F., K. H. Cook, E. K. Vizy, 2019: Changes in intense rainfall events and drought across Africa
738 in the 21st century. *Climate Dyn.*, 53, 2757-2777. doi:10.1007/s00382-019-04653-z.

739 He, B., S. Yang, and Z. Li, 2016: Role of atmospheric heating over the South China Sea and
740 western Pacific regions in modulating Asian summer climate under the global warming
741 background. *Climate Dyn.*, 46, 2897-2908.

742 He, S., S. Yang, and Z. Li, 2017: Influence of latent heating over the Asian and western Pacific
743 monsoon region on Sahel summer rainfall. *Sci. Reports*, 7, 7680,
744 <https://doi.org/10.1038/s41598-017-07971>.

745 Held, I. M. and B. J. Soden, 2006: Robust responses of the hydrological cycle to global warming.
746 *J. Climate*, **19**, 5686–5699.

747 Herman, R. J., A. Giannini, M. Biasutti, and Y. Kushnir, 2019: The Effects of Anthropogenic and
748 Volcanic Aerosols and Greenhouse Gases on 20th Century Sahel Precipitation. *Scientific*
749 *Reports*, submitted.

750 Hilker, T., A. I. Lyapustin, C. J. Tucker, F. G. Hall, R. B. Myneni, Y. Wang, J. Bi, Y. M. de Moura,
751 and P. J. Sellers, 2014: Vegetation dynamics and rainfall sensitivity of the Amazon. *Proc.*
752 *Natl. Acad. Sci. USA*, **111**, 16041–16046, doi:10.1073/pnas.1404870111

753 Hill, S. A., 2019: Theories for Past and Future Monsoon Rainfall Changes. *Current Climate*
754 *Change Reports*, **5**, 160-171.

755 Hsu, P.-C., T. Li, H. Murakami and A. Kitoh, 2013: Future change of the global monsoon revealed
756 from 19 CMIP5 models. *J. Geophys. Res. Atmos.*, **118**, 1247–1260.

757 Huang, P., S.-P. Xie, K. Hu, G. Huang and R. Huang, 2013: Patterns of the seasonal response of
758 tropical rainfall to global warming, *Nature Geos.*, 6, 357-361.

759 Huang, X., T. Zhou, A. Dai, H. Li, C. Li, X. Chen, J. Lu, J.-S. von Storch, and B. Wu, 2020a: South
760 Asian summer monsoon projections constrained by the Interdecadal Pacific Oscillation.
761 *Science Advances*, **6**, eaay6546. DOI: 10.1126/sciadv.aay6546.

762 Huang, X., T. Zhou, A. Turner, A. Dai, X. Chen, R. Clark, J. Jiang, W. Man, J. Murphy, J. Rostron, B.
763 Wu, L. Zhang, W. Zhang, and L. Zou, 2020b: The recent decline and recovery of Indian
764 summer monsoon rainfall: relative roles of external forcing and internal variability. *J.*
765 *Climate*, Accepted 12 March 2020. doi: 10.1175/JCLI-D-19-0833.1

766 Huang, X., T. Zhou, W. Zhnag, J. Jiang, P. Li, Y. Zhao, 2019: Northern Hemisphere land monsoon
767 precipitation chnages in the twentieth century revealed by multiple Reanalysis datasets,
768 *Climate Dyn.*, <https://doi.org/10.1007/s00382-019-04982-z>

769 Jalihal, C., J. Srinivasan, and A. Chakraborty, 2019: Modulation of Indian monsoon by water
770 vapor and cloud feedback over the past 22,000 years. *Nature Communications*, **10**, 1–8,
771 doi:10.1038/s41467-019-13754-6.

772 Jiang, X., Y. Luo, D.-L. Zhang, and M. Wu, 2019: Urbanization Enhanced Summertime Extreme
773 Hourly Precipitation over the Yangtze River Delta, *J Climate*, Accepted.

774 Jiang Jie, Tianjun Zhou. 2019. Global monsoon responses to decadal sea surface temperature
775 variations during the twentieth century: Evidence from AGCM simulations. *Journal of*
776 *Climate*, doi: 10.1175/JCLI-D-18-0890.1

777 Jin, Q., Wang, C. A revival of Indian summer monsoon rainfall since 2002. *Nature Clim*
778 *Change* **7**, 587–594 (2017).

779 Jourdain, N. C., A. S. Gupta, A. S. Taschetto, C. C. Ummenhofer, A. F. Moise, and K. Ashok, 2013:
780 The Indo-Australian monsoon and its relationship to ENSO and IOD in reanalysis data

781 and the CMIP3/CMIP5 simulations. *Climate Dyn.*, **41**, 3073–3102, doi:10.1007/s00382-
782 013-1676-1. Kawase, H., A. Murata, R. Mizuta, H. Sasaki, M. Nosaka, M. Ishii, and I.
783 Takayabu, 2016: Enhancement of heavy daily snowfall in central Japan due to global
784 warming as projected by large ensemble of regional climate simulations. *Climatic*
785 *Change*, 139, 265-278, doi:10.1007/s10584-016-1781-3.

786 Kawase, H., Y. Imada, H. Sasaki, T. Nakaegawa, A. Murata, M. Nosaka, and I. Takayabu, 2019:
787 Contribution of historical global warming to local-scale heavy precipitation in western
788 Japan estimated by large ensemble high-resolution simulations. *J. Geophys. Res. Atmos.*,
789 124, 6093-6103, doi:10.1029/2018JD030155.

790 Kendon, E.J., Stratton, R.A., Tucker, S. *et al.* , 2019: Enhanced future changes in wet and dry
791 extremes over Africa at convection-permitting scale. *Nat Commun* **10**, 1794.
792 <https://doi.org/10.1038/s41467-019-09776-9>

793 Kirchmeier-Young, M. C., F. W. Zwiers, and N. P. Gillett, 2017: Attribution of Extreme Events in
794 Arctic Sea Ice Extent. *J. Climate*, **30**, 553–571.

795 Kitoh, A., H. Endo, K. Krishna Kumar, I. F. A. Cavalcanti, P. Goswami, and T. Zhou, 2013:
796 Monsoons in a changing world: a regional perspective in a global context. *J. Geophys.*
797 *Res.*, **118**, 3053–3065, doi:10.1002/jgrd.50258.

798 Kitoh, A., 2017: The Asian monsoon and its future change in climate models: a review. *J.*
799 *Meteor. Soc. Japan*, **95**, 7-33, doi:10.2151/jmsj.2017-002.

800 Knutson et al. 2019a: Tropical Cyclones and Climate Change Assessment: Part I. Detection and
801 Attribution. *Bull. Amer. Meteorol. Soc.* doi.org/10.1175/BAMS-D-18-0189.1

802 Knutson et al. 2019b: Tropical Cyclones and Climate Change Assessment: Part II. Projected
803 Response to Anthropogenic Warming. Bull. Amer. Meteorol. Soc.
804 doi.org/10.1175/BAMS-D-18-0194.1

805 Krishnan, R., T.P. Sabin, D.C. Ayantika, A. Kitoh, M. Sugi, H. Murakami, A.G. Turner, J.M. Slingo
806 and K. Rajendran, 2013: Will the South Asian monsoon overturning circulation stabilize
807 any further? *Clim.Dyn.*, **40**, 187–211.

808 Krishnan, R., T. P. Sabin, R. Vellore, M. Mujumdar, J. Sanjay, B. N. Goswami, F. Hourdin, J.-L.
809 Dufresne, and P. Terray, 2016: Deciphering the desiccation trend of the South Asian
810 monsoon hydroclimate in a warming world. *Climate Dyn.*, **47**, 1007–1027.

811 Lahmers, T. M., C. L. Castro, D. K. Adams, Y. L. Serra, J. J. Brost, and T. Luong, 2016: Long-term
812 changes in the climatology of transient inverted troughs over the North American
813 monsoon region and their effects on precipitation. *J. Climate*, **29**, 6037–6064.

814 Lau, W. K.-M., and K.-M. Kim, 2017: Competing influences of greenhouse warming and aerosols
815 on Asian summer monsoon circulation and rainfall, *Asia-Pac., J. Atmos. Sci.*, **53**, 181–
816 194.

817 Lee, J.-Y. and B. Wang, 2014: Future change of global monsoon in the CMIP5. *Climate Dyn.*, **42**,
818 101–119, doi:10.1007/s00382-012-1564-0.

819 Lee, J.-Y., K.-S. Yun, Y.-M. Yang, E.-S. Chung and A. Babu, 2019: Challenges in constraining future
820 change of global land precipitation in CMIP6 models. Presented at the WMO Workshop
821 on Monsoon Climate Change Assessment, 2-3 December 2019, Zhuhai, China.

822 Li, G., S.-P. Xie, Y. Du, and Y. Luo, 2016: Effects of excessive equatorial cold tongue bias on the
823 projections of tropical Pacific climate change. Part I: the warming pattern in CMIP5
824 multi-model ensemble. *Climate Dyn.*, **47**, 3817–3831.

825 Li, J., and B. Wang, 2018: Origins of the decadal predictability of East Asian land summer
826 monsoon rainfall. *J. Climate*, **31**, 6229–6243.

827 Li, J., Z. Wu, Z. Jiang, and J. He, 2010: Can global warming strengthen the East Asian summer
828 monsoon? *J. Climate*, **23**, 6696-6705.

829 Li, W., Fu, R., 2006: Influence of cold air intrusions on the wet season onset over Amazonia. *J.*
830 *Climate*, **19**, 257–275, doi:10.1175/JCLI3614.1.

831 Li, X., J. Yu, and Y. Li, 2013: Recent Summer Rainfall Increase and Surface Cooling over Northern
832 Australia since the Late 1970s: A Response to Warming in the Tropical Western Pacific. *J.*
833 *Climate*, **26**, 7221–7239, doi:10.1175/JCLI-D-12-00786.1.

834 Li, Z., W. K. M. Lau, V. Ramanathan, et al., 2016: Aerosol and monsoon climate interactions over
835 Asia. *Reviews of Geophysics*, 54(1-4), 866-929.

836 Li, Z., Y. Sun, T. Li, Y. Ding, and T. Hu, 2019: Future changes in East Asian summer monsoon
837 circulation and precipitation under 1.5° C to 5° C of warming. *Earth's Future*, accepted.

838 Liebmann, B., M. P. Hoerling, C. Funk, I. Bladé, R. M. Dole, D. Allured, X. Quan, P. Pegion, and J.
839 K. Eischeid, 2014: Understanding recent Horn of Africa rainfall variability and change. *J.*
840 *Climate*, **27**, 8629–8645, doi:10.1175/JCLI-D-13-00714.1.

841 Lin, L., Z. Wang, Y. Xu, Q. Fu, and W. Dong, 2018: Larger Sensitivity of Precipitation Extremes to
842 Aerosol Than Greenhouse Gas Forcing in CMIP5 Models. *J. Geophys. Res. Atmos.*, **123**,
843 8062–8073. doi:10.1029/2018JD028821.

844 Liu, J., B. Wang, Q. H. Ding, X. Y. Kuang, W. Soon, and E. Zorita, 2009: Centennial variations of
845 the global monsoon precipitation in the last millennium: results from ECHO-G model. *J.*
846 *Climate*, **22**, 2356–2371, doi:10.1175/2008JCLI2353.1.

847 Liu, J., B. Wang, M. A. Cane, S.-Y. Yim and J.-Y. Lee, 2013: Divergent global precipitation changes
848 induced by natural versus anthropogenic forcing. *Nature*, **493**, 656–659.

849 Lodoun, T., A. Giannini, P. S. Traoré, L. Somé, M. Sanon, M. Vaksman, and J. M. Rasolodimby,
850 2013: Changes in seasonal descriptors of precipitation in Burkina Faso associated with
851 late 20th century drought and recovery in West Africa. *Environmental Development*, **5**,
852 96–108.

853 Luong, T. M., C. L. Castro, H.-I Chang, T. Lahmers, D. K. Adams, and C. A. Ochoa-Moya, 2017: The
854 more extreme nature of North American monsoon precipitation in the southwestern
855 U.S. as revealed by a historical climatology of simulated severe weather events. *J. Appl.*
856 *Meteor. Climatol.*, **56**, 2509–2529.

857 Ma, S., T. Zhou, D. A. Stone, D. Polson, A. Dai, P. A. Stott, H. von Storch, Y. Qian, C. Burke, P. Wu,
858 L. Zou, and A. Ciavarella, 2017: Detectable anthropogenic shift toward heavy
859 precipitation over eastern China. *J. Climate*, **30**, 1381-1396.

860 Maher, N. and Coauthors, 2019: The Max Planck Institute Grand Ensemble: Enabling the
861 exploration of climate system variability. *J. Advances in Modeling Earth Systems*, **11**,
862 2050–2069.

863 Maidment, R. I., R. P. Allan, and E. Black, 2015: Recent observed and simulated changes in
864 precipitation over Africa. *Geophys. Res. Lett.*, **42**, 8155–8164,
865 doi:10.1002/2015GL065765.

866 Malhi, Y., J. T. Roberts, R. A. Betts, T. J. Killeen, W. Li, and C. A. Nobre, 2008: Climate change,
867 deforestation, and the fate of the Amazon. *Science*, **319**, 169–172,
868 doi:10.1126/science.1146961.

869 Maloney, E.D., Adames, Á.F. & Bui, H.X. Madden–Julian oscillation changes under
870 anthropogenic warming. *Nature Clim Change* **9**, 26–33 (2019).
871 <https://doi.org/10.1038/s41558-018-0331-6>

872 Marvel, K., M. Biasutti, and C. Bonfils, 2019: Fingerprints of external forcing agents on Sahel
873 rainfall. *Environ. Res. Lett.*, revised version submitted and available for download in the
874 ESSOAr repository: <https://doi.org/10.1002/essoar.10502593.1>

875 Moon, S., and K. J. Ha, 2017: Temperature and precipitation in the context of the annual cycle
876 over Asia: Model evaluation and future change. *Asia-Pacific J. Atmos. Sci.*, **53**, 229–242,
877 doi:10.1007/s13143-017-0024-5.

878 Murphy, J. M., B. B. Booth, C. A. Boulton, R. T. Clark, G. R. Harris, J. A. Lowe and D. M. H. Sexton,
879 2014: Transient climate changes in a perturbed parameter ensemble of emissions-
880 driven earth system model simulations. *Climate Dyn.*, **43**, 2855–2885,
881 doi:10.1007/s00382-014-2097-5.

882 Nam, C., S. Bony, J.-L. Dufresne, and H. Chepfer, 2012: The ‘too few, too bright’ tropical low-
883 cloud problem in CMIP5 models. *Geophys. Res. Lett.*, **39**, L21801.

884 Nguyen, H., A. Evans, C. Lucas, I. Smith, and B. Timbal, 2013: The Hadley circulation in
885 reanalyses: Climatology, variability, and change. *J. Climate*, **26**, 3357–3376.

886 Nicholls, N., C. Landsea, and J. Gill, 1998: Recent trends in Australian region tropical cyclone
887 activity. *Meteorol. Atmos. Phys.*, **65**, 197–205.

888 Nigam, S., Y. Zhao, A. Ruiz-Barradas and T. Zhou, 2015: The South-Flood North-Drought pattern
889 over eastern China and the drying of the Gangetic Plain. *Chao*. 22 in *Climate Change:
890 Multidecadal and Beyond*. Eds. C.P. Chang, M. Ghil, M. Latif, J. M. Wallace. World
891 Scientific Series on Asia-Pacific Weather and Climate, Vol. 6, World Scientific, Singapore.
892 347-359. doi: 10.1142/9789814579933_0022.

893 Oh, H., K.-J. Ha, and A. Timmermann, 2018: Disentangling impacts of dynamic and
894 thermodynamic components on late summer rainfall anomalies in East Asia, *J. Geophys.
895 Res.*, **123**, 8623–8633, doi:10.1029/2018JD028652.

896 Omondi, P., L. A. Ogallo, R. Anya, J. M. Muthama, J. Ininda, 2013: Linkages between global sea
897 surface temperatures and decadal rainfall variability over Eastern Africa region. *Int. J.
898 Climatol.*, **33**, 2082–2104.

899 Panthou, G., T. Vischel, and T. Lebel, 2014: Recent trends in the regime of extreme rainfall in
900 the Central Sahel. *Int. J. Climatol.*, **3**, 3998–4006.

901 Pascale, S., W. R. Boos., S. Bordoni., T. L. Delworth, S. B. Kapnick, H. Murakami¹, G. A. Vecchi,
902 and W. Zhang, 2017: Weakening of the North American monsoon with global warming.
903 *Nat. Clim. Change*, **7**, 806–812.

904 Pascale, S., L. M. Carvalho, D. K. Adams, C. L. Castro, and I. F. A. Cavalcanti, 2019: Current and
905 future variations of the monsoons of the Americas in a warming climate, *Curr. Clim.
906 Change Rep.*, **5**, 125–144.

907 Polson, D., M. Bollasina, G. C. Hegerl, and L. J. Wilcox, 2014: Decreased monsoon precipitation
908 in the Northern Hemisphere due to anthropogenic aerosols. *Geophys. Res. Lett.*, **41**,
909 6023–6029. doi:10.1002/2014GL060811.

910 Prein, A. F., R. M. Rasmussen, K. Ikeda, C. Liu, M. P. Clark, and G. J. Holland, 2016: The future
911 intensification of hourly precipitation extremes. *Nature Climate Change*, **7**, 48–52.

912 Privé, N. C. and R. A. Plumb, 2007: Monsoon dynamics with interactive forcing. Part I:
913 Axisymmetric studies. *J. Atmos. Sci.*, **64**, 1417–1430.

914 Richardson, T. B., P. M. Forster, T. Andrews, O. Boucher, G. Faluvegid, D. Fläschner, Ø.
915 Hodnebrog, M. Kasoar, A. Kirkevåg, J.-F. Lamarque, G. Myhre, D. Olivié, B. H. Samset, D.
916 Shawki, D. Shindell, T. Takemura, and A. Voulgarakis, 2018: Drivers of precipitation
917 change: An energetic understanding. *J. Climate*, **31**, 9641–9657.

918 Rotstayn, L. D., W. Cai, M. R. Dix, G. D. Farquhar, Y. Feng, P. Ginoux, M. Herzog, A. Ito, J. E.
919 Penner, M. L. Roderick, M. and Wang, 2007: Have Australian rainfall and cloudiness
920 increased due to the remote effects of Asian anthropogenic aerosols? *J. Geophys. Res.*,
921 **112**, D09202, doi:10.1029/2006jd007712.

922 Roxy, M. K., K. Ritika, P. Terray, R. Murtugudde, K. Ashok, and B. N. Goswami, 2015: Drying of
923 Indian subcontinent by rapid Indian Ocean warming and a weakening land-sea thermal
924 gradient. *Nature Communications*, **6**, 7423, doi:10.1038/ncomms8423.

925 Roxy, M. K., Ghosh, S., Pathak, A., Athulya, R., Mujumdar, M., Murtugudde, R., ... & Rajeevan,
926 M., 2017: A threefold rise in widespread extreme rain events over central India. *Nature*
927 *communications*, **8**, 708.

928 Sabeerali, C., and R. Ajayamohan, 2017: On the shortening of Indian summer monsoon season
929 in a warming scenario. *Climate Dynamics*, 1-16.

930 Salzmann, M., 2016: Global warming without global mean precipitation increase? *Sci. Adv.*, **2**,
931 e1501572.

932 Salzmann, M., H. Weser, and R. Cherian, 2014: *J. Geophys. Res. Atmos.* **119**, 11321-11337.

933 Salzmann, M., and R. Cherian, 2015: On the enhancement of the Indian summer monsoon
934 drying by Pacific multidecadal variability during the latter half of the twentieth century.
935 *J. Geophys. Res. Atmos.* **120**(18), 9103-9118.

936 Sanogo, S., A. H. Fink, J. A. Omotosho, A. Ba, R. Redl, and V. Ermert, 2015: Spatio-temporal
937 characteristics of the recent rainfall recovery in West Africa. *Int. J. Climatol.*, **35**, 4589–
938 4605.

939 Sarr, M. A., M. Zoromé, O. Seidou, C. R. Bryant, and P. Gachon, 2013: Recent trends in selected
940 extreme precipitation indices in Senegal—A changepoint approach. *J. Hydrology*, **505**,
941 326–334.

942 Seth, A., S. A. Rauscher, M. Biasutti, A. Giannini, S. J. Carmargo and M. Rojas, 2013: CMIP5
943 projected changes in the annual cycle of precipitation in monsoon regions. *J. Climate*,
944 **26**, 7328–7351, doi:10.1175/JCLI-D-12-00726.1.

945 Sharmila, S., S. Joseph, A. Sahai, S. Abhilash, and R. Chattopadhyay, 2015: Future projection of
946 Indian summer monsoon variability under climate change scenario: An assessment from
947 CMIP5 climate models. *Global and Planetary Change*, **124**, 62–78.

948 Shawki, D., Voulgarakis, A. , Chakraborty, A., Kasoar, M., and J. Srinivasan, 2018: The South
949 Asian monsoon response to remote aerosols: Global and regional mechanisms, *J.*
950 *Geophys. Res., Atmospheres*, **123**, 11, 585–11,601.

951 Shi., H., B. Wang, Cook, E. D., J. Liu, and F. Liu, 2018: Asian Summer Precipitation over the Past
952 544 Years Reconstructed by Merging Tree Rings and Historical Documentary Records. *J.*
953 *Climate*, **31**, 7845-7861. DOI: 10.1175/JCLI-D-18-0003.1.

954 Shonk, J. P., A. G. Turner, A. Chevuturi, L. Wilcox, A. J. Dittus, and E. Hawkins, 2019: Uncertainty
955 in aerosol radiative forcing impacts the simulated global monsoon in the 20th century.
956 *Geophys. Res. Letts.*, revised version submitted. The latest version of this paper can be
957 accessed at [https://livereadingac-](https://livereadingac-my.sharepoint.com/:f/g/personal/a_g_turner_reading_ac_uk/E18hjGgHjs5KooEbLEP0IIIBGgSajLIwumiN9ARCV7IJNQ?e=GrH4NI)
958 [my.sharepoint.com/:f/g/personal/a_g_turner_reading_ac_uk/](https://livereadingac-my.sharepoint.com/:f/g/personal/a_g_turner_reading_ac_uk/E18hjGgHjs5KooEbLEP0IIIBGgSajLIwumiN9ARCV7IJNQ?e=GrH4NI)
959 [E18hjGgHjs5KooEbLEP0IIIBGgSajLIwumiN9ARCV7IJNQ?e=GrH4NI](https://livereadingac-my.sharepoint.com/:f/g/personal/a_g_turner_reading_ac_uk/E18hjGgHjs5KooEbLEP0IIIBGgSajLIwumiN9ARCV7IJNQ?e=GrH4NI).

960 Singh, M. S., Z. Kuang, and Y. Tian, 2017: Eddy influences on the strength of the Hadley
961 circulation: Dynamic and thermodynamic perspectives. *J. Atmos. Sci.*, **74**, 467–486.

962 Singh, D., S. Ghosh, M. K. Roxy, and S. McDermid, 2019: Indian summer monsoon: Extreme
963 events, historical changes, and role of anthropogenic forcings. *WIREs Clim. Change*,
964 e571, doi:10.1002/wcc571.

965 Sigmond, M., and J. C. Fyfe, 2016: Tropical Pacific impacts on cooling North American winters.
966 *Nature Climate Change*, **6**, 970–974.

967 Skansi, M. M., M. Brunet, J. Sigró, E. Aguilar, J. A. A. Groening, O. J. Bentancur, Y. R. C. Geier, R.
968 L. C. Amaya, H. Jácome, A. M. Ramos, C. O. Rojas, A. M. Pasten, S. S. Mitro, C. V.
969 Jiménez, R. Martínez, L. V. Alexander, P.D. Jones, 2013: Warming and wetting signals
970 emerging from analysis of changes in climate extreme indices over South America.
971 *Global and Planetary Change*, 100, 295-307. doi:10.1016/j.gloplacha.2012.11.004.

972 Sobel, A. H., and J. D. Neelin, 2006: The boundary layer contribution to intertropical
973 convergence zones in the quasi-equilibrium tropical circulation model framework.
974 *Theor. Comput. Fluid Dyn.*, **20**, 323–350.

975 Sontakke NA, Singh N, Singh HN (2008) Instrumental period rainfall series of the Indian region
976 (AD 1813-2005): Revised reconstruction, update and analysis. *Holocene* 18:1055–1066.
977 <https://doi.org/10.1177/0959683608095576>

978 Sooraj, K., P. Terray, and P. Xavier, 2016: Sub-seasonal behaviour of Asian summer monsoon
979 under a changing climate: Assessments using CMIP5 models. *Climate Dyn.*, **46**, 4003–
980 4025.

981 Sperber, K. R., H. Annamalai, I.-S. Kang, A. Kitoh, A. Moise, A. Turner, B. Wang, and T. Zhou,
982 2013: The Asian summer monsoon: an intercomparison of CMIP5 vs. CMIP3 simulations of
983 the late 20th century. *Climate Dyn.*, **41**, 2711-2744.

984 Taylor, C. M., D. Belušić, F. Guichard, D. J. Parker, T. Vischel, O. Bock, P. P. Harris, S. Janicot, C.
985 Klein, and Panthou, G., 2017: Frequency of extreme Sahelian storms tripled since 1982
986 in satellite observations. *Nature*, **544**, 475–478.

987 Taylor, C. M., A. H. Fink, C. Klein, D. J. Parker, F. Guichard, P. P. Harris, and K.R. Knapp, 2018:
988 Earlier seasonal onset of intense mesoscale convective systems in the Congo Basin since
989 1999. *Geophys. Res. Lett.*, **45**, 13458–13467, doi:10.1029/2018GL080516.

990 Timbal, B. and W. Drosowsky, 2013: The relationship between the decline of South Eastern
991 Australia rainfall and the strengthening of the sub-tropical ridge. *Int. J. Clim.*, **33**, 1021–
992 1034.

993 Turner, A. G., G. S. Bhat et al., 2019: Interaction of Convective Organisation with Monsoon
994 Precipitation, Atmosphere, Surface and Sea: the 2016 INCOMPASS field campaign in
995 India. *Quarterly Journal of the Royal Meteorological Society*, doi: 10.1002/qj.3633.

996 Vera, C. S., and L. Diaz, 2015: Anthropogenic influence on summer precipitation trends over
997 South America in CMIP5 models. *Int. J. Climatol.*, **35**, 3172–3177, doi:10.1002/joc.4153.

998 Wang, B., and Q. Ding, 2006: Changes in global monsoon precipitation over the past 56
999 years. *Geophys. Res. Lett.*, **33**, L06711, doi: 10.1029/2005GL025347.

1000 Wang, B., and Q. Ding, 2008: Global monsoon: Dominant mode of annual variation in the
1001 tropics. *Dynamics of Atmos. and Ocean, special issue 2*, doi:
1002 10.1016/j.dynatmoce.2007.05.002.

1003 Wang, B., C. Jin, and J. Liu, 2019: Future change of global monsoon projected by CMIP6 models.
1004 *J Climate*, Revised version submitted.

1005 Wang, B., Liu J, Kim HJ, Webster PJ, and Yim SY, 2012: Recent Change of the Global Monsoon
1006 Precipitation (1979-2008). *Climate Dyn.*, **39**, 1123-1135, doi: 10.1007/s00382-011-1266-
1007 z.

1008 Wang, B., J. Liu, H.-J. Kim, P. J. Webster, S.-Y. Yim, and B. Xiang, 2013: Northern Hemisphere
1009 summer monsoon intensified by mega-El Nino/southern oscillation and Atlantic
1010 multidecadal oscillation. *Proc. Nat. Acad. Sci.*, **110**, 5347–5352.

1011 Wang, B., S.-Y. Yim, J.-Y. Lee, J. Liu, and K.-J. Ha, 2014: Future change of Asian-Australian
1012 monsoon under RCP 4.5 anthropogenic warming scenario. *Climate Dyn.*, **42**, 83–100.

1013 Wang, B., J. Li, M.A. Cane, J. Liu, P.J. Webster, B. Xiang, H.-M. Kim, J. Cao, and K.-J. Ha,
1014 2018: Toward predicting changes in land monsoon rainfall a decade in advance. *J.*
1015 *Climate*, **31**, 2699–2714.

1016 Wang, P.-X., B. Wang, H. Cheng, J. Fasullo, Z. T. Guo, T. Kiefer, Z. Y. Liu, 2014: The Global
1017 Monsoon across Time Scales: Is there coherent variability of regional
1018 monsoons? *Climate of the Past.*, 10, 2163-2291.

1019 Wang, P.-X., B. Wang, H. Cheng, J. Fasullo, Z. Guo, T. Kiefer, and Z. Liu, 2017: The Global
1020 Monsoon across Time Scales: Mechanisms and Outstanding Issues. *Earth Science*
1021 *Reviews*, 174, 82-121.

1022 Willetts, P. D., J. H. Marsham, C. E. Birch, D. J. Parker, S. Webster, and J. Petch, 2017: Moist
1023 convection and its upscale effects in simulations of the Indian monsoon with explicit and
1024 parametrized convection. *Q. J. R. Meteorol. Soc.*, 143, 1073-1085, doi:10.1002/qj.2991.

1025 Wright, J. S., R. Fu, J. R. Worden, S. Chakraborty, N. E. Clinton, C. Risi, Y. Sun and L. Yin,
1026 2017: Rainforest-initiated wet season onset over the southern Amazon. *Proceedings of*
1027 *the National Academy of Sciences*, 114(32).

1028 Wu, M., Y. Luo, F. Chen, and W. K. Wong, 2019: Observed link of extreme hourly precipitation
1029 changes to urbanization over coastal South China. *J. Appl. Meteor. Climatol.*, 58, 1799-
1030 1819, doi:10.1175/JAMC-D-18-0284.1.

1031 Yang, Y., L. M. Russell, S. Lou, H. Liao, J. Guo, Y. Liu, B. Singh, and S. J. Ghan, 2017: Dust-wind
1032 interactions can intensify aerosol pollution over eastern China. *Nature Communications*,
1033 **8**, 15333, doi:10.1038/ncomms15333.

1034 Yin, L., R. Fu, E. Shevliakova, and R. E. Dickinson, 2013: How well can CMIP5 simulate
1035 precipitation and its controlling processes over tropical South America? *Climate Dyn.*,
1036 **41**, 3127–3143, doi:10.1007/s00382-012-1582-y.

1037 Ying, J., P. Huang, T. Lian, and H. Tan, 2019: Understanding the effect of an excessive cold
1038 tongue bias on projecting the tropical Pacific SST warming pattern in CMIP5 models.
1039 *Climate Dyn.*, **52**, 1805–1818.

1040 Yuan, X., S. Wang, and Z.-Z. Hu 2018: Do climate change and El Niño increase likelihood of
1041 Yangtze River extreme rainfall? [in “Explaining Extreme Events of 2016 from a Climate
1042 Perspective”]. *Bull. Amer. Meteor. Soc.*, 99 (1), S113-S117. doi: 10.1175/BAMS-D-17-
1043 0089.1.

1044 Zelinka, M. D., T. A. Myers, D. T. McCoy, S. Po-Chedley, P. M. Caldwell, P. Ceppi, S. A. Klein, and
1045 K. E. Taylor, 2020: Causes of higher climate sensitivity in CMIP6 models. *Geophysical
1046 Research Letter*, 47, e2019GL085782.

1047 Zhang, W., T. Zhou, L. Zhang, and L. Zou, 2019: Future intensification of the water cycle with an
1048 enhanced annual cycle over global land monsoon regions. *J. Climate*, **32**, 5437–5452.

1049 Zhang, W., T. Zhou, L. Zou, L. Zhang, and X. Chen, 2018: Reduced exposure to extreme
1050 precipitation from 0.5°C less warming in global land monsoon regions. *Nat. Commun.*,
1051 <https://doi.org/10.1038/s41467-018-05633-3>.

1052 Zhang, W., Zhou, T. 2019: Significant increases in extreme precipitation and the associations
1053 with global warming over the global land monsoon regions. *Journal of Climate*,
1054 <https://doi.org/10.1175/JCLI-D-18-0662.1>.

1055 Zheng, F., J. P. Li, and T. Liu, 2014: Some advances in studies of the climatic impacts of the
1056 Southern Hemisphere annular mode. *J. Meteor. Res.*, 28, 820-835.

1057 Zhou, T., D. Gong, J. Li, and B. Li, 2009: Detecting and understanding the multi-decadal
1058 variability of the East Asian Summer Monsoon – Recent progress and state of affairs.
1059 *Meteorologische Zeitschrift*, **18**, 455–467.

1060 Zhou, L. M., Y. H. Tian, R. B. Myneni, P. Ciais, S. Saatchi, Y. Y. Liu, S. L. Piao, H. S. Chan, E. F.
1061 Vermote, and co-authors, 2014: Widespread decline of Congo rainforest greenness in the
1062 past decade. *Nature*, **509**, 86–89, doi:10.1038/nature13265.

1063 Zhou, T., J. Lu and W. Zhang, 2020a: The sources of uncertainty in the projection of global land
1064 monsoon precipitation. *Geophys. Res. Lett.*, under review. Pdf file available at:
1065 https://drive.google.com/open?id=1hkuL4G_xQ-2B6PBYGSMHXDhBrcAARaPZ.

1066 Zhou T., W. Zhang, L. Zhang, X. Zhang, Y. Qian, D. Peng, S. Ma, B. Dong, 2020b: The dynamic
1067 and thermodynamic processes dominating the reduction of global land monsoon
1068 precipitation driven by anthropogenic aerosols emission. *Science China: Earth Sciences*,
1069 accepted and in press.

1070 Zhu, C. W., B. Wang, W. H. Qian, and B. Zhang, 2012: Recent Weakening of Northern East Asian
1071 Summer Monsoon: A Possible Response to Global Warming. *Geophys. Res. Lett.*, **39**,
1072 L09701, doi: 10.1029/2012GL051155.

1073

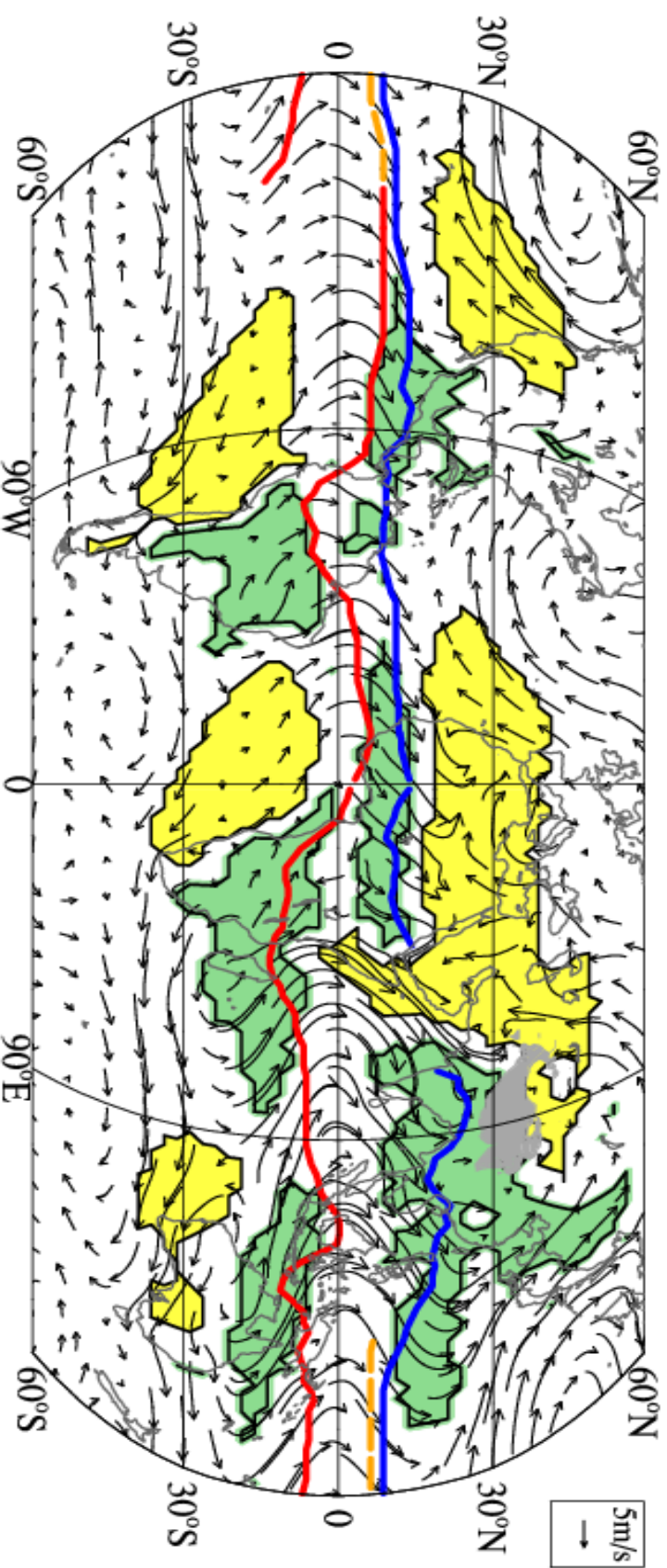


Figure 1. The GM precipitation domain (in Green) defined by the local summer-minus-winter precipitation rate exceeds 2 mm day⁻¹, and the local summer precipitation exceeds 55 % of the annual total (Wang and Ding 2008). Summer denotes May through September for the Northern Hemisphere and November through March for the Southern Hemisphere. The dry regions (in yellow) is defined by local summer precipitation being less than 1 mm day⁻¹. The arrows show August-minus-February 925 hPa winds. The blue (red) lines indicate the ITCZ position in August (February). Adopted from P.X. Wang et al. (2014).

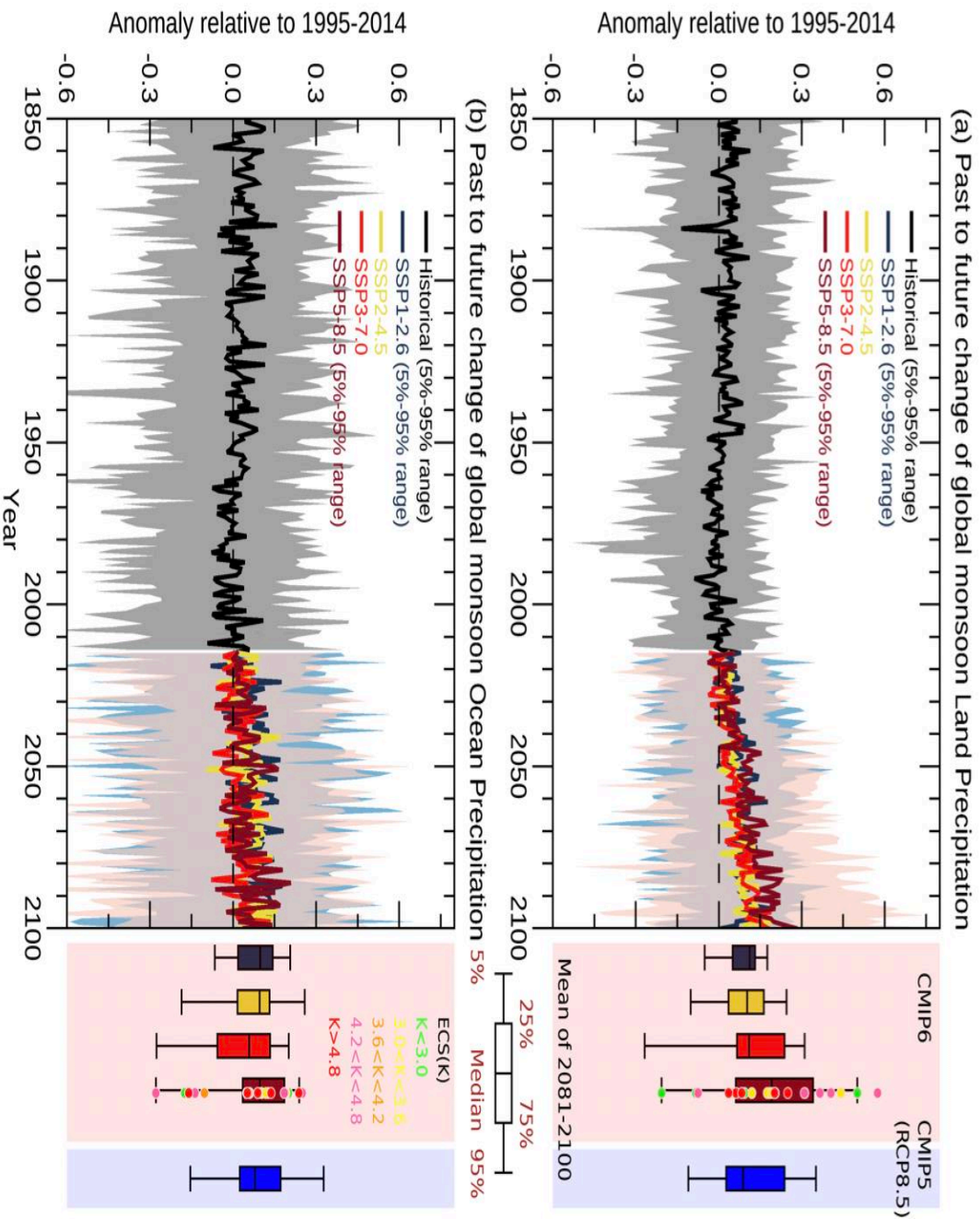


Fig. 2 Past to future changes of annual-mean global monsoon precipitation (mm/day) over (a) land and (b) ocean relative to the recent past (1995-2014) in historical simulation (1850-2014) and four core SSPs (2015-2100) obtained from 34 CMIP6 models. Pink and mid-blue shading indicate 5%-95% likely range of precipitation change in low emission (SSP1-2.6) and high emission (SSP5-8.5) scenario, respectively. The mean change during 2081-2100 relative to the recent past is also shown with the box plot in right-hand side obtained from four SSPs in 34 CMIP6 models compared to RCP 8.5 in 40 CMIP5 models. The solid dot in the box plot for SSP5-8.5 indicates individual model's equilibrium climate sensitivity (ECS).

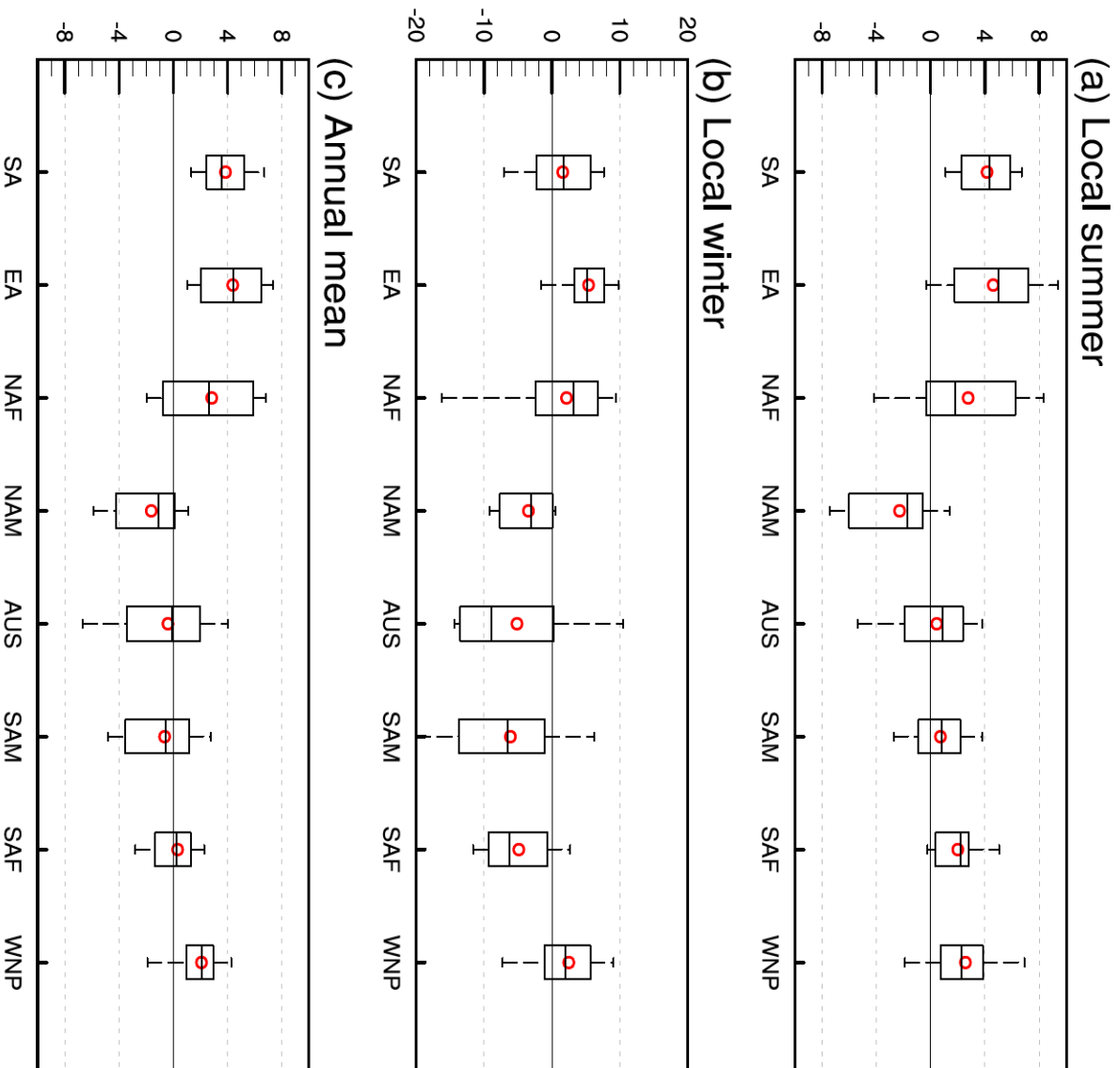


Fig. 3 Projected regional land monsoon precipitation sensitivity under the SSP2-4.5, i.e., the percentage change (2065–2099 relative to 1979–2013) per 1°C global warming, in units of $\%/\text{C}$) derived from 24 CMIP6 models for (a) local summer, (b) local winter, and (c) annual mean land monsoon precipitation for each region. Local summer means JJA in NH and DJFM for SH, and local winter means the opposite. The upper edge of the box represents the 83th percentile and the lower edge is the 17th percentile, the box contains 66% of the data. The horizontal line within the box is the median. Red circle is the mean. The vertical dash line segments represent the range of nonoutliers (5%-95%).

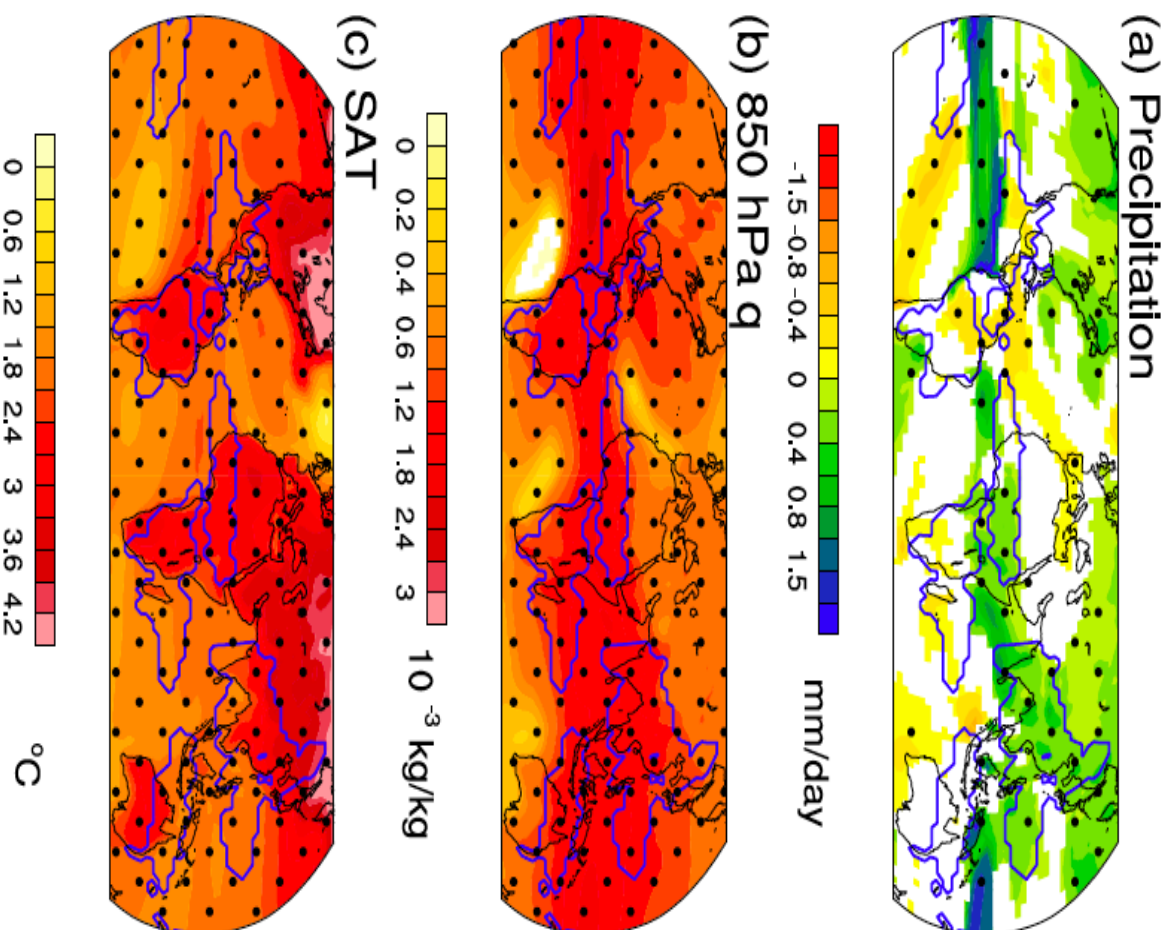


Fig. 4 Changes in the annual mean (a) precipitation, (b) 850 hPa specific humidity, and (c) surface air temperature. Changes are measured by the SSP2-4.5 projection (2065–2099) relative to the historical simulation (1979–2013) in the 15 models' MME. The color shaded region denotes the changes are statistically significant at the confidence level (likely change). Stippling denotes areas where the significance exceeds 95% confidence level (very likely) by student t-test.

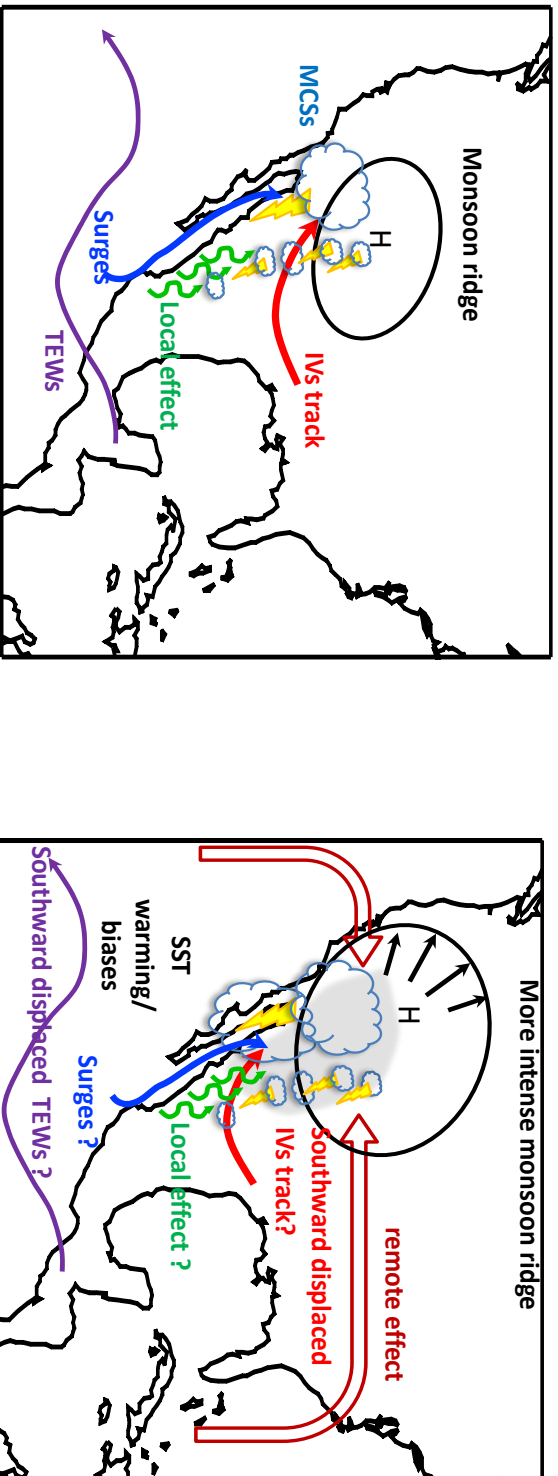


Fig. 5: Schematic main features related to present (left panel) and future (right panel) changes for the North American Monsoon (left). The expansion and northwestward shift of the NAM ridge, the southward shift of the upper-level inverted troughs (IVs) track, and the strengthening of the remote stabilizing effect due to SST warming are shown. Red and blue shading indicates drying and wetting respectively due to the large-scale shifts. Larger clouds in the lower panel is suggestive of more intense MCS-type convection. A question mark (?) on the lower panels indicates uncertainty in the response, as it is the case, for example, for the local mechanisms associated with atmosphere-land interaction, NAM moisture surges and southward shift the tropical easterly waves (TEWS) track.

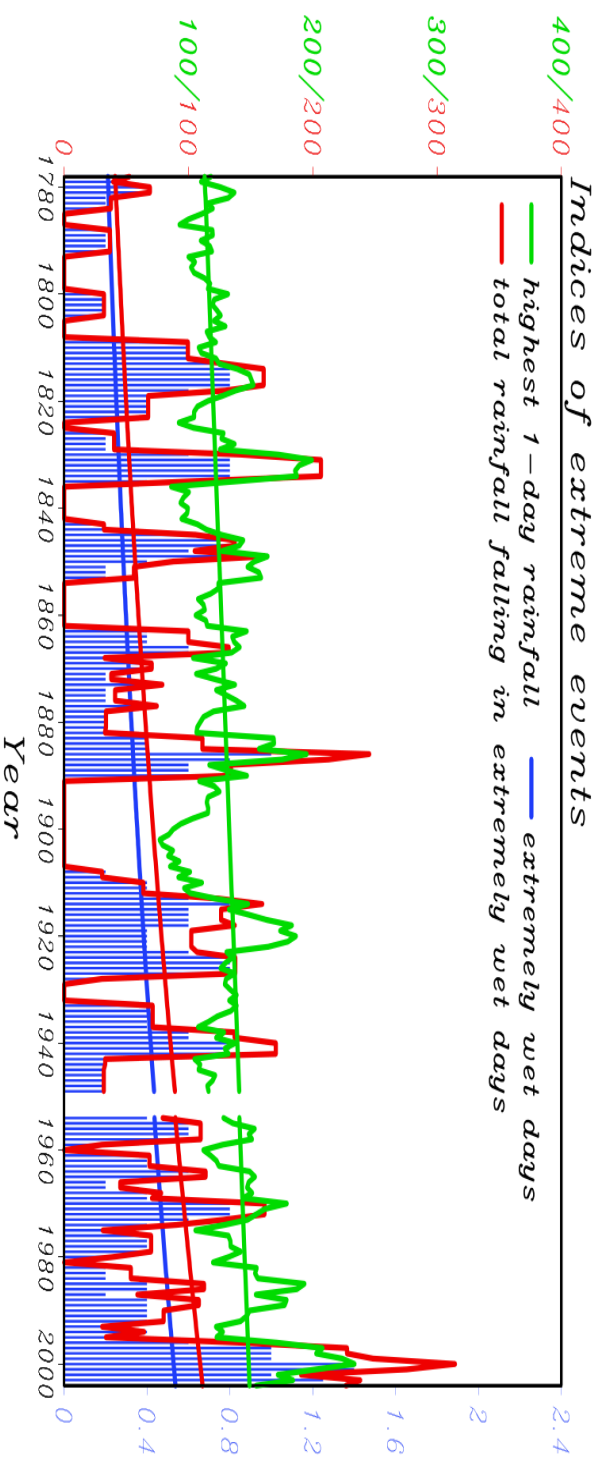


Figure 6. **Time series of extreme precipitation events observed at Seoul, Korea since 1778.** Running five-year means of the summer highest one-day precipitation amount (green, mm/day in the left y-axis), the number of extremely wet days (blue, right y-axis) and the precipitation amount falling in the extremely wet days (red, mm/day in the left axis). The extremely wet days are calculated as the 99th percentile of the distribution of the summer daily precipitation amount in the 227-year period. Also shown are the corresponding trends obtained by least-square regression for the green curve and logistic regression for the blue and red curve. Adopted from Wang et al. (2006)

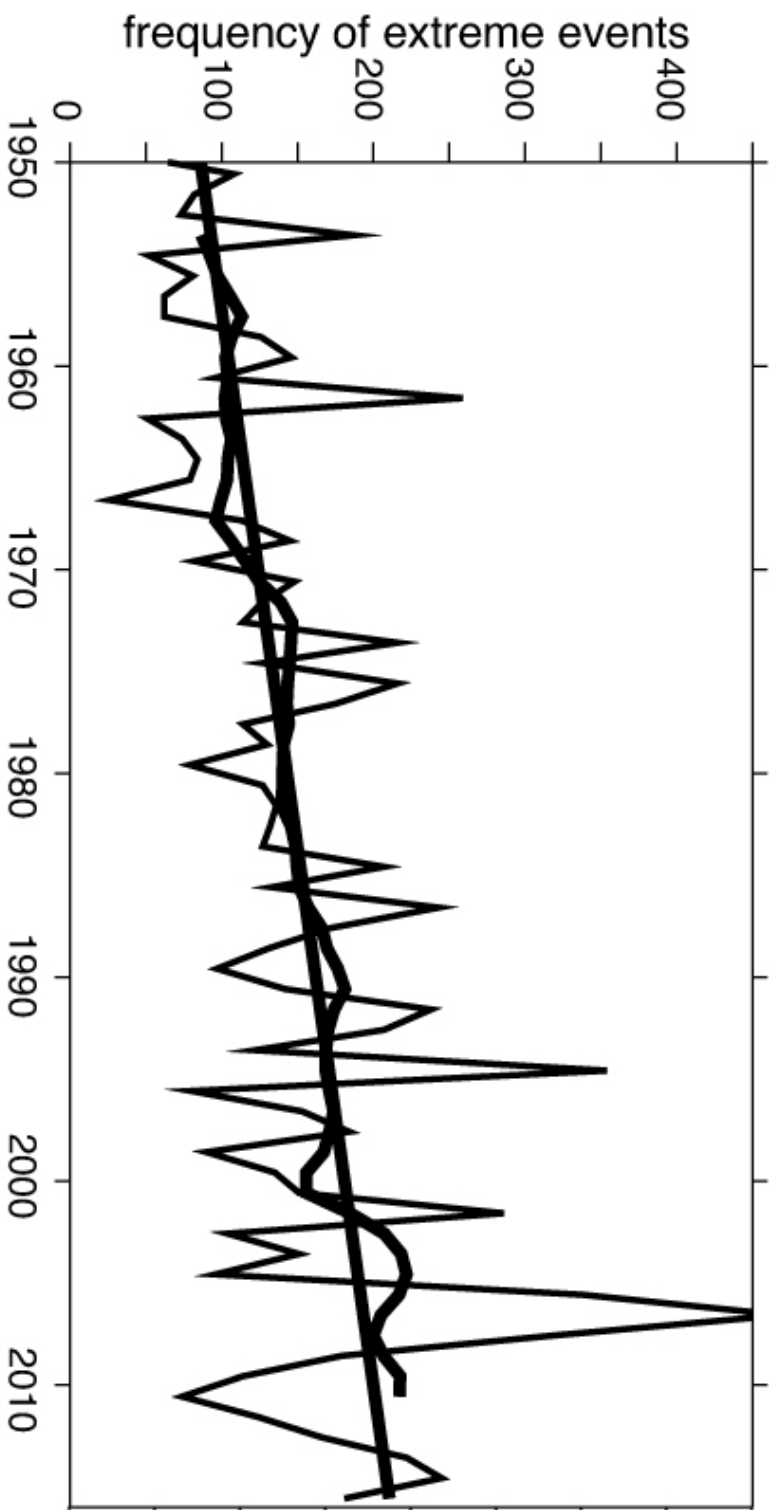
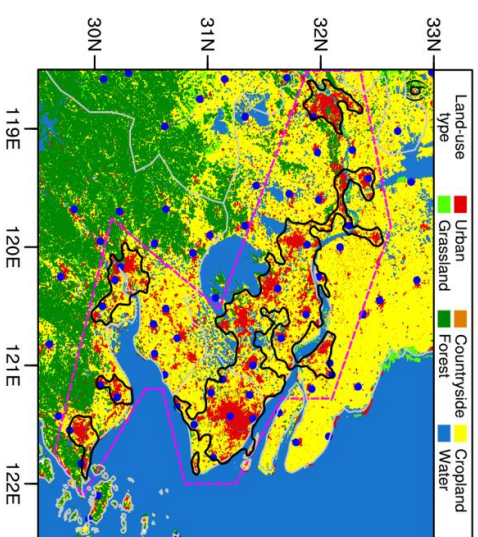
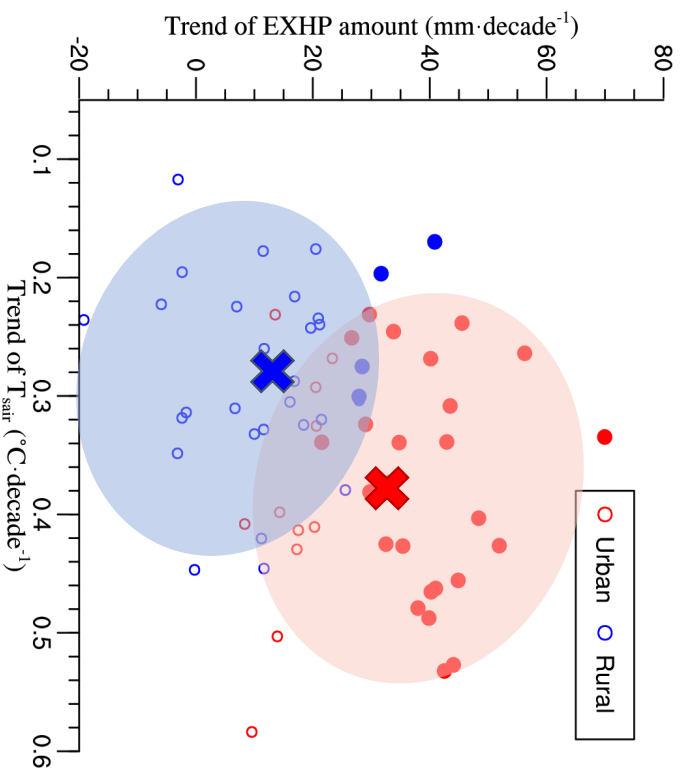


Figure 7. Frequency of extreme rain events (number of grid cells exceeding 150 mm/day per year) over central Indian subcontinent (75°–85° E, 19°–26° N) for the summer monsoon (June–September) during 1950–2015. The trend lines shown in the figures are significant at 95% confidence level. The smoothed curves on the time series analyses represent 10-year moving averages. Adopted from Roxy et al. (2017).



	Mean trends	T_{sair} ($^{\circ}\text{C}\cdot\text{decade}^{-1}$)	EXHP amount ($\text{mm}\cdot\text{decade}^{-1}$)
Rural		0.28	12.8
Urban		0.38	32.6

Figure 8 The surface air temperature and extremely hourly rainfall trends for urban stations (red) and rural stations (blue) in the Yangzi River Delta, calculated from changes from 1975-1996 to 1997-2018, during MJJAS. The thick crosses are averages of the station values. Adapted from Figs. 1 and 11 in Jiang et al. (2020)

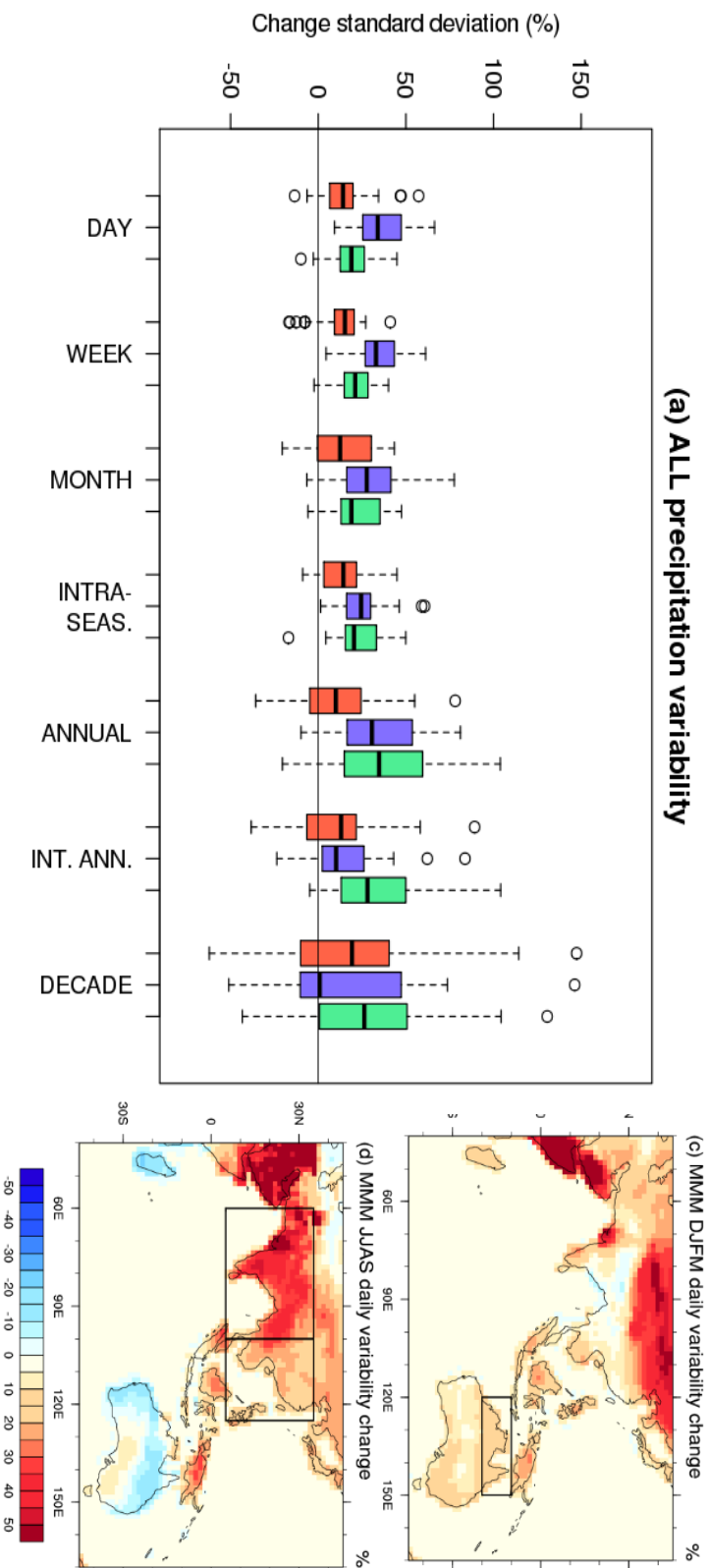


Fig. 9 (a) RCP8.5 (2050-2100) minus HIST (1950-2000) differences in band-pass-filtered daily rainfall standard deviation (%) for Australian (red, left boxes), South Asian (purple, center boxes) and East Asian (green, right boxes) monsoon domain. Data are DJFM months for AUS and JJAS months for SA and EA. Daily data are band-pass-filtered for the set of bands indicated on the x-axis. (c) and (d) are the multi-model mean change in standard deviation of *daily* rainfall (%) from HIST (1950-2000) to RCP8.5 (2050-2100) in (c) DJFM and (d) JJAS. The South Asian (SA), East Asian (EA) and Australian (AUS) monsoon domains are shown in the relevant wet season. (from Brown et al. 2017).